CONFÉRENCIERS

P. Armbruster
G.F. Bertsch
J.-P. Blaizot
X. Campi
B. Desplanques
A.H. Mueller
U. Mosel
B. Mottelson
P. Paul
C.J. Pethick
B. Pire
P. Radvanyi
C. Rubbia
R.H. Siemssen
G. Sletten
M. Spiro
B. Tamain
S. Vervier
W. Weise

UJFG

LES HOUCHES

SESSION LXVI

30 Juillet – 30 Août 1996

OÙ EN EST LA PHYSIQUE NUCLÉAIRE APRÈS 100 ANS D'EXISTENCE ?

TRENDS IN NUCLEAR PHYSICS, 100 YEARS LATER

édité par

H. NIFENECKER, J.-P. BLAIZOT, G.F. BERTSCH
W. WEISE *et* F. DAVID

1998

ELSEVIER
Amsterdam – Lausanne – New York – Oxford – Shannon – Singapore – Tokyo

COURSE 3

NUCLEAR COLLECTIVE MOTION

G.F. Bertsch

Department of Physics and Institute for Nuclear Theory, University of Washington, Seattle, WA 98195 U.S.A.

H. Nifenecker, J.-P. Blaizot, G.F. Bertsch, W. Weise and F. David, eds.
Les Houches, Session LXVI, 1996
Où en est la physique nucléaire après 100 ans d'existence?
Trends in Nuclear Physics, 100 Years Later

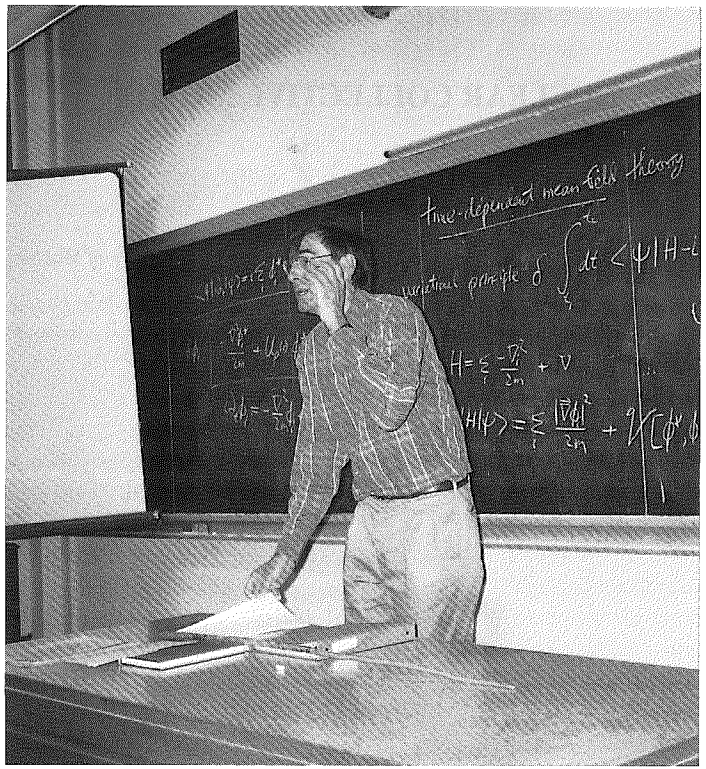

Contents

0. Note to the reader

These lecture notes are intended as introductory, emphasizing the theoretical tools and the qualitative phenomena. Thus, they may be useful to readers in other fields who would like to see the phenomena and models of another discipline of quantum many-particle physics. As in other fields, nuclear theory advances through lengthy numerical calculations, but I believe that the computer-generated numbers are only trustworthy and useful if they can be understood in simple terms. It is this simplified essence I have tried to extract from theory, leaving out unessential details. The material is mostly well-known to nuclear theorists. However, there are a few new derivations may be pointed out here. In eq. (3.1–3.9), I derive the collective oscillation frequency from a general variational principle, which shows explicitly the connection to time-dependent mean-field theory. Also new is eq. (6.3) for the particle escape width.

1. Introduction

How does a nucleus respond to an external perturbation? This fundamental question of nuclear physics is the subject of these lectures. In the early history of nuclear physics, the dynamics was thought to be purely statistical, since that theory described well the behavior of fission at low energies. Just as the emergence of single-particle motion with the shell model was a surprise in 1947, it was a surprise when collective behavior was discovered in the nuclear response. The first such mode, the giant dipole vibration, was discovered in 1947 (although there were hints about this behavior much earlier). It is shown in Fig. 1, which has graphed the photon absorption cross section for various isotopes of neodymium as a function of energy. The lowest curve, for the isotope ^{142}Nd, shows a smooth curve peaking at 14.9 MeV. This is the resonance. It is very well fitted by the Lorentzian function, see Section 2 below. As I will show in these lectures, we have a very good understanding now of some aspects of the resonance, but not all.

Over the years several other giant resonances were discovered, when experimental probes became available that were sensitive to the modes. These are listed

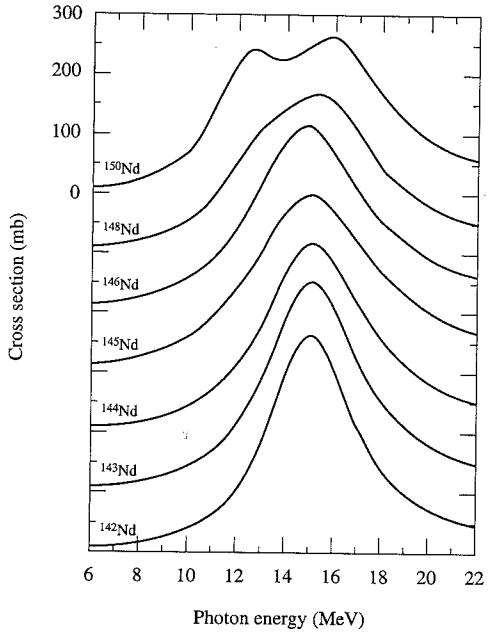

Fig. 1. The giant dipole resonance in isotopes of neodinium, from ref. [?]. The lowermost graph, showing the photon absorption cross section for ^{142}Nd, is well-described by a Lorentzian function, eq. (2.2), with parameters $\omega = 14.9$ MeV, $\gamma = 4.4$ MeV and a total strength of 1.2 times the TRK sum-rule, eq. (2.11). The splitting of the peak in other isotopes is discussed in Section 2.1.1.

in Table 1. The giant dipole has isospin $T = 1$, and spin-parity $J^P = 1^-$, which couples easily to the electromagnetic field. Thus the dipole was discovered in photon absorption experiments. The next mode, the quadrupole, has isospin $T = 0$, which allows it to couple strongly to the nuclear field of heavy ion projectiles. In fact the early identification of this mode came from inelastic scattering of protons and of electrons. The monopole mode in Table 1 also has isospin $T = 0$ and the same parity as the quadrupole, which makes it somewhat difficult to distinguish from the quadrupole by inelastic scattering. Nevertheless there are characteristic features in the angular distributions* of inelastic scattering that led to a clear identification by 1978. The Gamow–Teller mode is rather different in that it is an excitation of the spin degrees of freedom, and it also involves changing a neutron into a proton. The reaction that is specific to this mode is hadronic charge exchange such as the (p,n) reaction.

* Unfortunately, there is not enough time in my lectures to explain these characteristics of the angular distributions.

Table 1
A gallery of giant resonances

Resonance	Discovery date	Quantum numbers $T(J^P)$	Frequency
Dipole	1947	1 (1^-)	$79/A^{1/3}$ MeV
Quadrupole	1972	0 (2^+)	$65/A^{1/3}$
Gamow-Teller	1976	1 (1^+)	
Monopole	1978	0 (0^+)	$80/A^{1/3}$
Mie		(1^-)	$4\pi e^2 n/3m_e$

Although the giant resonances were discovered many years ago, their study continues to be an active area of research. A reference for recent work is the conference proceedings [1]. Earlier work is reviewed in ref. [2].

The last resonance listed in Table 1 is not in nuclear physics. It is the collective oscillation of the electrons in a spherical metallic cluster. Its analogies with the nuclear giant dipole resonance are so strong that I can't resist including it in the table.

In the giant resonances we find very clearly the interplay between single-particle motion and collective behavior. We shall see that these modes are very simple in a certain sense — the nuclear wave function may be very complicated, but its subtleties fortunately play a small role in the dynamics. To discuss giant resonances, I shall first review the theoretical tools we can bring to bear on the problem. One important theme is that mean field theory gives a good starting point for the discussion, although it is obviously incomplete.

For the most part, these lectures will be based on the monograph I wrote with R. Broglia, "Oscillations in Finite Quantum Systems" [3]. Two other books I particularly recommend on the subject are Bohr and Mottelson's "Nuclear Structure, Vol. II" [4], and Ring and Schuck's "The Nuclear Many-Body Problem" [5].

2. Theoretical tools

2.1. The response function

Before going through the quantum mechanical definitions of the response function, it is instructive to remind ourselves that the concept is classical as well. We shall often see the Lorentzian function as a profile of the response to a sinusoidal external field. It is useful to know where this function comes from. It certainly cannot be derived in a natural way in treating the quantum-mechanical nuclear Hamiltonian. It arises as purely classical response, giving the behavior of an oscillator damped by a linear friction force. Thus, the starting point for the

Lorentzian is the equation of motion of a particle, by the driving force F_0.

$$m\frac{d^2x}{dt^2} + v\frac{dx}{dt} + kx = F_0 \cos\omega t \tag{2.1}$$

The response is the amplitude of motion of the system divided by the external force F_0. I will not bother writing down the two components, proportional to $\sin\omega t$ and $\cos\omega t$. The Lorentzian function arises when one calculates the power absorbed by the oscillator. This is given by

$$P = \frac{F_0^2}{m}\frac{\gamma\,\omega^2}{(\omega^2-\omega_0^2)^2+\gamma^2\omega^2} \tag{2.2}$$

where $\omega_0 = \sqrt{k/m}$ is the natural frequency in the absence of damping and $\gamma = v/m$ is the damping rate.

In quantum mechanics we can define a response in a very similar way. The starting point is a stationary wave function for the quantum system

$$H|\psi_0\rangle = E_0|\psi_0\rangle \tag{2.3}$$

Corresponding to the external force in eq. (2.1), we perturb the system with an external field. Consider a potential field with a sinusoidal time dependence $V_0\cos(\omega t)$. Then the wave function in first-order perturbation theory is*

$$|\psi\rangle = |\psi_0\rangle - \sum_n |\psi_n\rangle\Big(\frac{e^{i\omega t}}{E_{n0}-\omega} + \frac{e^{-i\omega t}}{E_{n0}+\omega}\Big)\langle\psi_n|V_0/2|\psi_0\rangle \tag{2.4}$$

where $E_{n0} = E_n - E_0$ is the excitation energy of the state $|\psi_n\rangle$. We next find the expectation of an operator S in this state. This corresponds to finding the classical amplitude of motion in eq. (2.1). Often S will be simply a function of position. When taking a matrix element of single-particle operator in a multiparticle state, a summation over particles is always implicit. Assuming that the expectation of S vanishes in the ground state, the expectation value in the perturbed state is

$$\langle\psi|S|\psi\rangle_t = \sum_n \langle\psi_0|S|\psi_n\rangle\Big(\frac{1}{E_{n0}-\omega} + \frac{1}{E_{n0}+\omega}\Big)\langle\psi_n|V_0|\psi_0\rangle\cos(\omega t) \tag{2.5}$$

The coefficient of the cosine function is the quantum mechanical response. It is most frequently used with the same fields for the external potential as for the probe, $S = V_0$. We will write the response in this case as

$$\Pi_S = \sum_n \langle\psi_0|S|\psi_n\rangle\Big(\frac{1}{E_{n0}-\omega} + \frac{1}{E_{n0}+\omega}\Big)\langle\psi_n|S|\psi_0\rangle \tag{2.6}$$

* I will leave off factors of $\hbar$ in all equations.

We will need integrals over the response, and this requires a prescription for integrating around the poles in the above formula. The proper causal behavior is assured with the replacement $\omega \to \omega - i\eta$. We can then write down the imaginary part of the response using the identity

$$\lim_{\eta\to 0}\frac{1}{\omega - i\eta} = \frac{P}{\omega} + i\pi\delta(\omega) \tag{2.7}$$

The imaginary part of the response is closely related to the strength function, defined as

$$\mathcal{S}_S = \sum_n |\langle\psi_0|S|\psi_n\rangle|^2\delta(E_{n0}-\omega). \tag{2.8}$$

The relation is

$$\mathcal{S}_S = \frac{1}{\pi} Im\Pi_S(\omega). \tag{2.9}$$

2.2. *Sum rules*

Sum rules provide one of the most powerful tools to deal with quantum systems that cannot be treated exactly. The best known of these is the Thomas–Reiche–Kuhn (TRK) sum rule for the dipole strength function. For Hamiltonians with local interactions, the integral of the strength function multiplied by energy is given by

$$\sum_f \langle f|z|i\rangle^2\delta(\omega_i-\omega) = \int S_z(\omega)\,\omega\,d\omega = \frac{N_p}{2m}. \tag{2.10}$$

In this formula N_p is the number of particles in the system. The m is the mass of each particle. For some purposes it is convenient to combine the TRK sum rule with the formula for the dipole absorption cross section. The resulting formula for the energy-integrated cross section is

$$\int_0^\infty \sigma\,d\omega = \frac{2\pi^2e^2\hbar N_p}{mc}. \tag{2.11}$$

We have here included the factors of c and $\hbar$ because the formula is often applied with physical units.

There is an additional subtlety in nuclei associated with the nucleus's center-of-mass coordinate. If we apply the TRK sum rule to the protons in the nucleus, different states of the center-of-mass coordinate will be treated as part of the excitations. To get around this, one uses a dipole operator that has the center of mass explicitly subtracted out. The operator is given by

$$D = \frac{N}{A}\sum_p z_p - \frac{Z}{A}\sum_n z_n. \tag{2.12}$$

In this formula and later the symbols Z, N and $A = N+Z$ refer to the numbers of protons, neutrons and nucleons, respectively. With the operator D the factor N_p becomes ZN/A on the right-hand side of the TRK sum rule eq. (2.10). A simple derivation of this result without using the specific form of the internal dipole operator can be argued as follows. The total sum rule for the protons including the center-of-mass excitation is $Z/2m_N$, with m_N the nucleon mass. The contribution to the sum rule from the center-of-mass motion must be given by that for a particle of mass Am_N and charge Z, namely $Z^2/2Am_N$. The difference represents the internal excitations and given by

$$\sum_{\text{internal excitations } f} \langle f|z|i\rangle^2 \delta(\omega_i - \omega) = \frac{Z}{2m_N} - \frac{Z^2}{2Am_N} = \frac{1}{2m_N}\frac{ZN}{A} \tag{2.13}$$

Empirically, the giant dipole resonance shown in Fig. 1 has 120% of the sum rule, integrating over the peak up to an energy of 20 MeV. This shows that to an accuracy of 20%, the relevant degrees of freedom in nuclear physics are the neutrons and protons with their free masses. The deviation from a precise fulfillment of the sum rule may be due to momentum-dependent terms in the the Hamiltonian, or to other degrees of freedom such as pions and quarks that are neglected in the nonrelativistic nuclear many-body description. In fact these possibilities are not exclusive — when a Hamiltonian is simplified by integrating out some degrees of freedom, the reduced Hamiltonian in general will have energy- and momentum-dependent terms.

Exercise 1: Derive the cluster sum rule [6]. This sum rule is based on a model of the nucleus considered as two clusters of nucleons which are bound together. The sum rule gives the strength associated with the relative wave function between the two clusters. Ans.: The factor ZN/A becomes $(Z_1N_2 - Z_2N_1)^2/AA_1A_2$, where the particle numbers in the clusters are (Z_1, N_1, A_1) and (Z_2, N_2, A_2), and $A = A_1 + A_2$.

Exercise 2: In the nuclear dipole sum rule, how is it possible that the center-of-mass motion doesn't take care of itself? After all, the energy to excite the center of mass of a free particle is zero.

Exercise 3: Many of the lectures in the school here concern quark structure in nuclei, so one might suppose that an independent quark model could be a valid starting point for nuclear structure. Work out the sum rule for constituent quarks, expressed in units of m_N and A. The quarks have mass $m_q \approx m_N/3$ and charges $+2/3$ and $-1/3$, and there are three times as many of them as there are nucleons. You will see from the answer that nature hides these degrees of freedom in nuclear physics.

2.3. Mean field theory

Mean field theory is the big success story of theoretical physics. A huge list of phenomena in many-particle systems can be understood starting only with the assumption that the particles move independently in a common potential. For fermion systems, the mean field theory is obtained by minimizing the energy of a Hamiltonian in the space of Slater determinants. This is just Hartree–Fock theory. The formal starting point can be expressed succinctly as the variational principle

$$\frac{\delta\langle\psi|H|\psi\rangle}{\delta\phi_i} = 0, \tag{2.14}$$

where ϕ_i is a single-particle wave function in the Slater determinant,

$$\psi = \mathcal{A}\prod_i \phi_i(r_i).$$

Here the $\phi_i(r_i)$ are the single-particle wave functions. The object to be minimized, the Hartree–Fock energy, can be expressed in terms of the ϕ_i as

$$\langle\psi|H|\psi\rangle = \sum_i \int d^3r \frac{|\nabla\phi_i|^2}{2m} + \tag{2.15}$$

$$+\sum_{i<j}\int\int d^3r d^3r'\, \phi_i^*(r)\phi_j^*(r')\, v(r-r')\left(\phi_i(r)\phi_j(r') - \phi_i(r')\phi_j(r)\right)$$

The minimization gives Hartree–Fock equations which may be written as

$$-\frac{\nabla^2\phi_i}{2m} + U_{\rm d}\phi_i + \hat{U}_{\rm ex}\phi_i = \epsilon_i\phi_i$$

$$\text{with } U_{\rm d}(r) = \sum_i \int d^3r' |\phi_i(r')|^2 v(r-r')$$

$$\text{and } \hat{U}_{\rm ex}\phi_i = \sum_j \phi_j(r)\int d^3r'\, \phi_j^*(r')\phi_i(r')\, v(r-r').$$

The ϵ_i are the single-particle energies, and appear in the minimization as Lagrange multipliers to insure that the norm of the single-particle wave function is preserved. There are two potential fields in the above equation, a direct potential $U_{\rm d}$ and an exchange potential $\hat{U}_{\rm ex}$. The direct potential is a familiar object but the exchange potential is nonlocal and we have therefore written it as an operator. That indicates that the expression $\hat{U}_{\rm ex}\phi_i$ actually requires an integration rather than being a simple multiplication.

Exchange potentials are rather awkward to deal with in practice, and it is very common to replace them by local potentials. In molecular and condensed matter physics, this is called the Local Density Approximation (LDA). The direct potential is just the ordinary Coulomb field,

$$U_{\rm d}(r) = e^2 \int d^3r' \, \frac{n(r')}{|r - r'|} \tag{2.16}$$

where $n(r)$ is the number density of the charged particles. The exchange and correlation parts of the electron–electron interaction is commonly parameterized as [7]

$$V_{xc} = \frac{-0.916}{r_s(r)} - 0.0666 \quad G\left(\frac{r_s(r)}{11.4}\right), \quad r_s(r) = \left(\frac{3}{4\pi\, n(r)}\right)^{1/3} \tag{2.17}$$

and $G(x) = (1 + x^3)\, \ln(1 + \frac{1}{x}) - x^2 + \frac{x}{2} - \frac{1}{3}$.

This parameterization was obtained by fitting the energy of an electron gas calculated numerically. It includes effects of electron correlation as well as the exchange, so in some sense the LDA goes beyond Hartree–Fock.

In nuclear physics, the interaction is so strong that a real Hartree–Fock treatment would make no sense at all. Nevertheless, as in the same spirit of the condensed matter LDA, one can parameterize a Hamiltonian to be evaluated in mean field theory. Unlike the condensed matter LDA, the parameters in the Hamiltonian cannot be calculated to sufficient accuracy by first principles. So one ends up with a phenomenological theory in which the parameters of the Hamiltonian are adjusted to fit some set of properties of the many-particle system. I will mention three such Hamiltonians that have been widely applied, namely Skyrme, Gogny, and the relativistic mean field.

2.3.1. Skyrme Hamiltonian

The Skyrme Hamiltonian was originally applied to nuclear mean field theory in ref. [8]; examples of recent applications are ref. [9,10]. The interaction is based on contact potentials. We will see later that nuclei with normal properties cannot be derived from a Hamiltonian having only an ordinary delta-function potential, so additional terms depending on density and the momentum operator are included. The interaction of the Skyrme Hamiltonians may be written as

$$v = p(n, \tau_z, \sigma, \nabla_{12})\, \delta(r - r') \tag{2.18}$$

where p is a polynomial in its arguments. Of course it must satisfy the required symmetries, in particular, angular momentum, parity, and isospin. There are many Skyrme Hamiltonians on the market. They all give similar looking single-particle wave functions, but details of nuclear structure and binding energy differences far from stability are quite variable.

2.3.2. Gogny Hamiltonian

This Hamiltonian was proposed in ref. [11]; a recent application may be found in ref. [12]. It has contact terms similar to the Skyrme Hamiltonian, but the main part is a finite-range two-particle interaction. The finite range interaction is taken as a sum of two Gaussians with all possible spin and isospin exchange operators

$$V(r) = \sum_{i=1,2} (W_i + B_i P_\sigma - H_i P_\tau - M_i P_\sigma P_\tau) e^{-r^2/b_i^2}. \tag{2.19}$$

2.3.3. Relativistic mean field

The last model on the list is the relativistic mean field model, a model that was popularized by Serot and Walecka [13]. See ref. [14] for an example of a recent application to nuclear structure. The model makes use of potentials that transform relativistically as scalar and vector fields. The fields roughly correspond to the ω and σ mesons. The Hamiltonian is the Dirac Hamiltonian for the nucleons in the scalar-plus-vector mean field. The Lagrangian density has the form

$$\boldsymbol{L} = \bar{\psi}(\partial\!\!\!/ - g_\omega \phi\!\!\!/ - g_\sigma \sigma - m_N)\psi + \boldsymbol{L}(\omega) + \boldsymbol{L}(\sigma), \tag{2.20}$$

where the last two terms are free Lagrangian densities for the σ and ω fields. The Dirac–Hartree equation is simply

$$(i\partial\!\!\!/ - g_\omega \phi\!\!\!/ - g_\sigma \sigma - m_N)\psi_i = \epsilon_i \gamma_o \psi_i. \tag{2.21}$$

This is solved self-consistently together with the fields σ and ω. I won't write down the equations for the fields, but they are just the classical field equations, with the nucleon density and current as source terms.

The relativistic theory has two very nice features. First, the vector field introduces a momentum dependence into the mean field. The empirical single-particle potential is in fact momentum-dependent, and the sign of the potential, becoming less attractive at high momentum, is correctly predicted*. Second, it gives a spin-orbit field of correct sign and magnitude to explain spectroscopic spin-orbit splittings as well as polarizations in elastic scattering. The input coupling strengths and meson masses are adjusted to fit nuclear matter.

Counterbalancing these attractive properties are several undesirable features. The exchange is ignored completely, which is hard to justify with interactions that have the short ranges of the ω and σ mesons. The model is not truly consistent in a

* However, the strength of the momentum dependence is too large: the relativistic potential becomes strongly repulsive at high energy, rather than falling off to a small value, as required by the empirical potential.

relativistic sense, because the Dirac sea is ignored in most applications. When one includes the sea, the ugly problems of cutoffs and renormalization arise. Finally, the predicted incompressibility is far too high with the simplest form for the ω and σ terms in the Lagrangian density. That is usually patched up by adding additional terms to $\boldsymbol{L}(\sigma)$.

2.3.4. Which is best?

Each of these approaches has its merits — Skyrme is easily calculable, Gogny includes finite-range forces, and the relativistic model respects the spinor character of the nucleon field. All these models are similar, however, in that they reproduce the basic features of shell physics — magic numbers at 28, 50 and 126, and deformed ground states in the middle of shell closures. The magnitude of quadrupole deformation can even be calculated to about 10–20% accuracy in strongly deformed nuclei with any of these Hamiltonians. It remains a task for the future to apply the different models in a global way to the complete set of nuclides, and to see whether the physics omitted in the Skyrme parameterization plays any essential role in the ground state properties.

3. Time-dependent mean field theory

Time-dependent mean field theory (TDHF) is the extension of Hartree–Fock replacing the single particle energy ϵ_i in eq. (2.16) by the time derivative operator $i\partial_t$. The idea was introduced by Dirac in 1930 [15]. In nuclear physics, Rowe used the TDHF as a bridge to the Random Phase Approximation, (RPA) which is the main application. It is also of some value in the theory of heavy ion reactions, where it was first applied as a large amplitude theory in [16]. The usual starting point to derive TDHF is the following variational principle

$$\delta \int dt \langle\psi| i\partial_t - H|\psi\rangle = 0. \tag{3.1}$$

Here, as in eq. (2.14), ψ is the Slater determinant of single-particle orbitals ϕ_i. We shall not discuss the full TDHF, which becomes quickly numerically unwieldy, but only consider two specializations. The first is to collective motion, which requires that the motion in all of the single-particle orbitals be the same. The other specialization, RPA, keeps the freedom of individual orbitals but requires that the amplitude of the motion be small.

3.1. Collective motion

There are two kinds of collective motion in nuclei: the low frequency modes such as rotation and beta vibrations, and the giant vibrations at high frequency. I will discuss mainly the latter in these lectures. The high frequency limit is often called diabatic motion in contrast to adiabatic motion at low frequency. The theory of diabatic collective motion is quite elegant. One only need assume that giant resonances exist which satisfy the energy-weighted sum rule for some field $S(r)$. Let us consider the effect of $S(r)$ on the ground state. Applying the field at time $t = 0$, the ground state wave function ψ_0 is changed to

$$\psi(t = 0_+) = e^{iS}\psi_0. \tag{3.2}$$

The perturbed ψ is no longer an eigenstate of the Hamiltonian. Its initial time evolution, apart from an overall phase, is given by

$$\psi(t) = (1 + t[H, S] + \ldots)\psi(t = 0_+). \tag{3.3}$$

If the Hamiltonian has only local interactions, the commutator in the above equation involves only the kinetic energy operator,

$$[H, S] = [-\frac{\nabla^2}{2m}, S] = -\frac{\nabla^2 S}{2m} - \frac{\nabla S}{m} \cdot \nabla.$$

The density ρ then evolves in time as

$$\rho = \rho_0 + t\delta\rho$$

where

$$\delta\rho = \nabla \cdot \rho_0 \frac{\nabla S}{m} \tag{3.4}$$

is the collective transition density. Eq. 3.4 is closely related to the equation of continuity and is easy to understand physically. The field S gives the particles an initial velocity $\nabla S/m$. The product with ρ_0 is the current. Finally, the divergence of the current represents the rate at which the particle density changes.

A collective model can be built from the two operators, S and $[H, S]$. We define time-dependent coordinates $\alpha(t)$ and $\beta(t)$ with the construction

$$|\alpha\beta\rangle = e^{i\alpha S}\, e^{\beta[H,S]}\psi_0. \tag{3.5}$$

The dynamic equations will particularly involve the state with $\alpha = 0$, which I write as

$$|\beta\rangle = |\alpha = 0, \beta\rangle = e^{\beta[H,S]}\psi_0.$$

This is inserted in the variational principle to get the equations of motion for α and β. The variational principle is exactly the same as the usual one for a Lagrangian, so the equations of motion are just the equations that follow from a Lagrangian $\boldsymbol{L} = \langle\alpha\beta|i\partial_t - H|\alpha\beta\rangle$. After some nontrivial algebra, the equations can be reduced to the following [17]

$$\dot{\beta} = \alpha \tag{3.6}$$

$$\dot{\alpha}\partial_\beta\langle\beta|S|\beta\rangle + \partial_\beta\langle\beta|H|\beta\rangle + \frac{\alpha^2}{2m_N}\langle\beta|[S,[H,S]]|\beta\rangle = 0. \tag{3.7}$$

Exercise 4: Derive eq. (3.6) from the Lagrangian equation,

$$\frac{d}{dt}\frac{\partial \boldsymbol{L}}{\partial\dot{\alpha}} - \frac{\partial \boldsymbol{L}}{\partial\alpha} = 0 \tag{3.8}$$

with $\boldsymbol{L} = \langle\alpha\beta|i\partial_t - H|\alpha\beta\rangle$. Hint: the Lagrangian may be simplified to the following expression: $\boldsymbol{L} = -\dot{\alpha}\langle\Psi_\beta|S|\Psi_\beta\rangle - \langle\Psi_\beta|H|\Psi_\beta\rangle - \alpha^2\langle\Psi_\beta|[S,[H,S]]|\Psi_\beta\rangle/2m_N$.

The equations for α and β are nonlinear, but we can linearize them for small amplitudes. The resulting motion is of course harmonic, and the formula for the frequency comes out to be

$$\omega^2 = \frac{\langle\Psi_0|[[H,[H,S]],[H,S]]|\Psi_0\rangle}{\langle\Psi_0|[S,[H,S]]|\Psi_0\rangle} = \frac{M_3}{M_1}. \tag{3.9}$$

In the last equality I have expressed the numerator and denominator as energy-weighted moments of the transition strength [18],

$$M_n = \sum\langle 0|S|i\rangle^2(E_i - E_0)^n.$$

The numerator and denominator in eq. (3.9), multiplied by m_N^2, have physical interpretations as the spring constant and the inertia associated with the collective coordinate β. In fact, we may express these commutator expectation values in the following form

$$M = m_N^2\langle 0|[S,[H,S]]|0\rangle = \frac{m_N}{2}\langle 0||\nabla S|^2|0\rangle \tag{3.10}$$

$$K = m_N^2\langle\Psi_0|[[H,[H,S]],[H,S]]|\Psi_0\rangle = \partial_\beta^2\langle\beta|H|\beta\rangle\Big|_{\beta=0}. \tag{3.11}$$

The first expectation value is the kinetic energy associated with the velocity field S, and is thus the inertia. The second expression is the second derivative of the expectation of the Hamiltonian, and is thus the spring constant associated with the deformation. Eq. (3.9) for the frequency then has the familiar form

$$\omega^2 = \frac{K}{M}. \tag{3.12}$$

3.1.1. Application to giant dipole: Goldhaber–Teller mode

As a simple application of the diabatic theory, consider a simple uniform dipole field in which protons and neutrons move against each other in the x direction:

$$S = \tau_z x \tag{3.13}$$

The inertia is trivial to calculate; in eq. (3.10) we have $|\nabla S|^2 = |\tau_z|^2 = 1$ and get

$$M_D = m_N A. \tag{3.14}$$

To calculate the spring constant we have to know how the interaction changes when we uniformly move the protons away from the neutrons. We can make a very crude estimate if we assume that the densities are Gaussian and the interaction is a contact interaction. The Gaussian assumption is reasonable for light nuclei, which is the domain of applicability of the Goldhaber–Teller model. The neutron–proton interaction in the displaced state depends on β as

$$V(\beta) \sim V_0\int d^3r d^3r' \exp(-(r-\beta\hat{x})^2/2\sigma^2)\exp(-(r+\beta\hat{x})^2/2\sigma^2)\delta^3(r-r')$$

$$= e^{-\beta^2/\sigma^2}V_0\int d^3r e^{-r^2/\sigma^2}. \tag{3.15}$$

where V_0 is the total neutron–proton interaction energy at $\beta = 0$. It is easy to take the second derivative of this with respect to β to find the spring constant. The result is

$$K_D = \frac{2V_0}{\sigma^2} \tag{3.16}$$

and the collective frequency is given by

$$\omega_D^2 = \frac{2V_0}{A\sigma^2 m_N}. \tag{3.17}$$

To get a numerical estimate, we need to determine V_0 and σ. Let us consider the nucleus ^{16}O. The rms charge radius of the nucleus is 2.7 fm, which implies that $\sigma = 2.7/\sqrt{3} = 1.56$ fm. The total interaction energy may be estimated as the binding energy plus the kinetic energy, with the kinetic energy determined from the Fermi gas value. The binding energy of ^{16}O is 127 MeV, and the Fermi gas kinetic energy is about 22 MeV/nucleon. Thus the total interaction energy is $127 + 16\times 22 = 480$ MeV. Of this roughly half is associated with the neutron–proton interaction. This gives for the frequency

$$\omega_D \approx \sqrt{\frac{(480)(41.5)}{(16)(1.56)^2}} = 22.6\ \text{MeV} \tag{3.18}$$

This is a little bit low for the mean resonance energy. We have left out meson exchange currents which raise the energy and increase the sum rule (after all, the charged pions responsible for the exchange currents have a lighter mass than the nucleons!). The model of the dipole resonance based on the field eq. (3.13) was

proposed by Goldhaber and Teller in 1948. The A-dependence of the model is given by

$$\omega_D \sim A^{-1/6}. \tag{3.19}$$

This can be easily seen from the behavior of K and M. From eq. (3.14) the inertia increases linearly with A. The spring constant K is asymptotically proportional to the the surface area of the nucleus, because with a uniform drop there is no change in the interior density when neutrons are displaced with respect to protons. This implies $K \sim A^{2/3}$, giving for the oscillation frequency eq. (3.19).

As mentioned in the introduction, the giant dipole energy falls more quickly than $A^{-1/6}$ in heavy nuclei. There is another early model that displays $A^{-1/3}$ behavior, the hydrodynamic model of Steinwedel and Jensen. Here nuclei are viewed as uniform drops with sharp surfaces, and the neutron–proton counterflow vanishes at the surface. The uniformity of the interior implies that the velocity field is proportional to a spherical Bessel function. For a dipole oscillation along the z-axis, the field is

$$S(\boldsymbol{r}) = j_1(kr)\cos\theta. \tag{3.20}$$

The condition that the radial velocity vanishes at the surface is $\partial S/\partial r|_{r=R} = 0$, which gives the numerical condition

$$kR = 2.08. \tag{3.21}$$

One knows in hydrodynamics that ω is proportional to the wavenumber k, so we get $\omega \sim k \sim 1/R \sim A^{-1/3}$.

For completeness let us see how this result comes out of eq. (3.9). The inertia for the field eq. (3.20) is given by

$$M = \frac{m}{2}\int d^3r\,\rho(r)|\nabla S|^2 = -\frac{m}{2}\int d^3r\,\rho(r)S\nabla^2 S = -k^2\frac{m}{2}\int d^3r\,\rho(r)S^2. \tag{3.22}$$

In the second step, we integrated by parts making use of the boundary condition. The spring constant for the oscillation is obtained by assuming that the energy density varies quadratically with the isospin density,

$$\langle\beta|H|\beta\rangle = \frac{\beta^2}{2}\int d^3r\,v_\tau(\delta\rho_\tau)^2.$$

We use eq. (3.4) for the isospin density. The expression again simplifies after integrating by parts,

$$K = v_\tau\int d^3r\,(\nabla\cdot\rho_0\nabla S)^2 = \int d^3r\,v_\tau(\rho_0\nabla^2 S)^2 = k^4 v_\tau\int d^3r\,\rho_0^2 S^2. \tag{3.23}$$

Taking the ratio of K to M, we see that $\omega^2 \sim k^2$, giving the hydrodynamic relation between ω and k.

With its stiff boundary condition, the hydrodynamic model is too crude to explain the giant dipole resonance frequencies quantitatively*. Nevertheless, the qualitative behavior with frequency inversely proportional to size, $\omega \sim 1/R$, is dramatically displayed in the dipole response of deformed nuclei. The length R is the distance along the direction of oscillation; in deformed nuclei there are two inequivalent directions with different dipole resonance frequencies. This is seen in Fig. 1, which displays the dipole strength function for a range of isotopes of neodymium. The heavier isotopes are deformed and show a distinct split of the dipole into two components.

3.2. *RPA response*

The "random phase approximation" (RPA) is the small amplitude limit of TDHF. It may be derived by adding an external potential to the TDHF equations, and expanding the solution as a perturbation on the stationary wave functions. We shall use the response formulation with the density operator $\hat{\rho}(r)$ as the field. This will be sufficiently general to treat all local interactions. We first evaluate eq. (2.6) using the solutions of the static Hartree–Fock equations, with ψ_0 the ground-state Slater determinant and ψ_n excited Slater determinants. We need only consider ψ_n having a single orbital different from the ground state, because more complicated states will have vanishing matrix elements with the ground state. The matrix element is simply

$$\langle\psi_{ij}|\hat{\rho}(r)|\psi_0\rangle = \phi_j^*(r)\phi_i(r)$$

where the orbital i (the hole orbital) in the ground state is replaced by j (the particle orbital) in the excited state ψ_{ij}. Eq. (2.6) for the response reads

$$\Pi^0(r,r',\omega) = \tag{3.24}$$

$$\sum_i^{\text{occ}}\sum_j \phi_i^*(r)\,\phi_j(r)\,\phi_j^*(r')\phi_i(r') \times \left(\frac{1}{\epsilon_i-\epsilon_j-\omega}+\frac{1}{\epsilon_i-\epsilon_j+\omega}\right)$$

The density perturbation produced by an external field V is then given by

$$\delta\rho(r) = \int d^3r'\Pi^0(r,r',\omega)V(r') \tag{3.25}$$

* In their original paper [19], Steinwedel and Jensen made an adiabatic (rather than diabatic) estimate of K. This introduced a compensating error so their result was in good agreement with the empirical formula in Table 1.

which we write in operator notation as

$$\delta\rho = \Pi^0 V$$

The density fluctuation makes a change in the potential field, which acts then acts back on the density fluctuation again. To lowest order, the internal potential is changed by an amount $(\delta U/\delta\rho)\delta\rho$, and we can write

$$\delta\rho = \Pi^0\left(V + \frac{\delta U}{\delta\rho}\delta\rho\right) \tag{3.26}$$

We may now solve for $\delta\rho$

$$\Pi^{\mathrm{RPA}} = \left(1 - \Pi^{(0)}\frac{\delta U}{\delta\rho}\right)^{-1}\Pi^0 \tag{3.27}$$

This equation looks simple, but one should remember that it really is an integral equation. However, the equation reduces to an algebraic equation when the interaction is separable. This simplification will be discussed in Section 3.3 below.

There is another formulation of RPA as a matrix equation in the space of particle–hole configurations. This formulation is more general than eq. (3.27) in that it allows nonlocal interactions such as $\hat{U}_{\mathrm{ex}}$ to be included exactly. The response formulation only deals with the local density operator $\hat{n}(r)$, so the interactions may only depend on $n(r)$. For local interactions, the two formulations are entirely equivalent. The noninteracting response in the particle–hole representation is given by

$$\Pi^0 = \sum_{ij}|ij\rangle\frac{n_i - n_j}{\epsilon_i - \epsilon_j - \omega}\langle ij|$$

Note that the two energy denominators in eq. (3.25) are both contained in this formula due to the unrestricted sums over orbitals i and j, the combination (ij) giving one term and (ji) the other. In ref. [3] it is shown that the poles of eq. (3.27) with this form for the unperturbed response may be found by diagonalizing the matrix equation

$$\begin{pmatrix} A & B \\ B & A \end{pmatrix}\begin{pmatrix} X \\ Y \end{pmatrix} = \omega\begin{pmatrix} X \\ -Y \end{pmatrix} \tag{3.28}$$

where the matrices A and B and the vectors X and Y are in the space of particle–hole states $|ph\rangle$. The matrix elements are given by $\langle ph|A|p'h'\rangle = \langle ph|dU/d\rho|p'h'\rangle + (\epsilon_p - \epsilon_h)\delta_{pp'}\delta_{hh'}$. and $\langle ph|B|p'h'\rangle = \langle ph|dU/d\rho|h'p'\rangle$.

We can go from the matrix formulation, eq. (3.28), to the response formulation by identifying the eigenvalues with the poles of Π^{RPA}. To make a connection between the two formulations in the other direction, the particle–hole amplitudes

Table 2

Comparison of the response formulation and the particle–hole configuration space formulation of RPA.

Method	Computational effort	Relative advantage
Response	N^3	fast; exact continuum
Configuration	N^6	exact exchange and nonlocal interaction

X and Y may be calculated directly from the response if the pole energies ω_α and the transition potential δU_α are known. The relations are

$$X_a(ph) = -\frac{\langle p|\delta U|h\rangle}{\epsilon_p - \epsilon_n - \omega_\alpha} \tag{3.29}$$

$$Y_a(ph) = -\frac{\langle h|\delta U|p\rangle}{\epsilon_p - \epsilon_n + \omega_\alpha}.$$

As mentioned above, the matrix formulation in particle–hole configuration space is more general in that it permits nonlocal interactions to be included in the Hamiltonian. However, there are two disadvantages of the matrix formulation that should be mentioned. One is the numerical effort. In either formulation, the time-consuming task is inverting or diagonalizing a matrix, which increases with dimensionality M as M^3. In the case of the response function, the dimensionality is essentially the size of a vector needed to represent a wave function — perhaps amplitudes on a lattice in coordinate space. This increases as the size of the system N, so the overall effort scales as N^3. In contrast, the particle–hole configuration space has a dimensionality that scales as N^2 for a space large enough to respect the sum rules. Here the overall scaling is then N^6. Another advantage of the response function method is that the continuum can be treated exactly. This comes about because the free response is constructed from single-particle Green's functions, and there is a well-known analytic formula for a Green's function in the continuum. These relative merits and disadvantages are summarized in Table 2.

3.3. Separable interactions

The RPA becomes extremely simple when the interaction is separable. By this is meant that the interaction can be expressed in the form

$$v(r_1, r_2) = \kappa f(r_1) f(r_2). \tag{3.30}$$

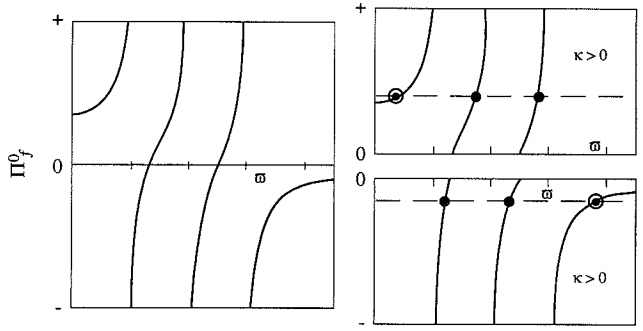

Fig. 2. The RPA dispersion relation, eq. (3.32). The upper left graph shows the solution when the interaction is attractive. The circled solution lies at a frequency below the lowest particle–hole state (seen as divergence in the curve at $\omega = 1$. The lower curve shows the solution for repulsive interactions. In this case the collective solution, shown as the circle, lies above the highest particle–hole state.

The simplification comes about because of a mathematical identity for inverting dyadic matrices*. The identity reads

$$(1 - |\xi\rangle\langle\eta|)^{-1} = 1 + \frac{|\xi\rangle\langle\eta|}{1 - \langle\eta|\xi\rangle}. \tag{3.31}$$

To derive the RPA for separable interactions, we write the response in a particle–hole representation. The product $\Pi^0 v$ is expressed

$$\Pi^0 v = \sum_{ij} |ij\rangle \frac{n_i - n_j}{\epsilon_i - \epsilon_j - \omega} \langle ij|f\rangle \kappa f(r).$$

This matrix has a dyadic structure, implying for the polarization

$$(1 - \Pi^0 v)^{-1} = 1 + \Pi^0 \frac{1}{1 - \kappa \sum_{ij} (n_i - n_j)|\langle ij|f\rangle|^2/(\epsilon_i - \epsilon_j - \omega)}.$$

The resonances occur where the denominator vanishes; that condition is given by the RPA dispersion relation

$$\sum_{ij} \frac{n_i - n_j}{\epsilon_i - \epsilon_j - \omega} |\langle ij|f\rangle|^2 = \frac{1}{\kappa} \tag{3.32}$$

It is easy to see the qualitative behavior of the collective states from the RPA dispersion relation. The right hand side of eq. (3.32) is sketched in Fig. 2. When $\kappa < 0$ corresponding to a repulsive interaction, the equality may be satisfied with

* A dyadic matrix is one that can be expressed as the outer product of two vectors, i.e. its matrix elements have the form $A_{ij} = u_i v_j$.

a pole at high frequency. The stronger the interaction, the higher the pole will be. Conversely, if $\kappa > 0$ corresponding to an attractive interaction, there will be a pole below the lowest particle–hole energy. As the interaction is increased in strength, the pole moves down to zero energy and disappears into the complex plane. In that situation, the mean-field ground state is unstable.

Historical note. The RPA was originally proposed by Bohm and Pines [20] as a theory of the plasmon in an infinite electron gas. There the excitations can be characterized by the momentum k that they carry. Making a Fourier transform of the Coulomb interaction, the important component is the Fourier component matching the momentum of the excitation,

$$v(r_1 - r_2) = e^{ikr_1} e^{-ikr_2} \frac{4\pi e^2}{k^2} + \cdots$$

It may be seen that this is separable allowing the frequency of the mode to be calculated by eq. (3.32). The other Fourier components do not contribute coherently in the integrals. They are neglected because of their "random phases", hence the designation RPA.

3.3.1. An example: the giant dipole

An example of the application of separable interactions is the following treatment of the giant dipole mode, taken from ref. [3]. The function f has to be an isovector function and dipolar. We simply take a linear function, of opposite sign for neutrons and protons. If the oscillation is in the x direction, we will only need the term

$$v(r_1, r_2) = \kappa x_1 \tau_z(1) x_2 \tau_z(2).$$

To determine the strength κ, we go to empirical data on the static nuclear potential. The single-particle potential has a well-known isospin dependence; it may be parameterized as

$$U_\tau = \tau_z V_\tau \frac{N - Z}{A},$$

with $V_\tau \approx 26$ MeV. We assume that the potential is due to the local difference in neutron and protons densities, so that we can write for an arbitrary isovector density ρ_τ

$$\delta V = V_\tau \rho_\tau / \rho_0. \tag{3.33}$$

Let us take the isovector density to have the form $\rho_\tau = cx\tau_z\rho_0$. We then calculate δV using

$$\delta V = \int d^3r' v(r, r') \delta\rho(r')$$

and compare with eq. (3.33). The result is

$$\kappa_D = \frac{3V_\tau}{A\langle r^2\rangle}.$$

Once we have the interaction, it is a simple matter to write down the RPA dispersion relation. In this case eq. (3.32) becomes

$$\sum_{ph} \frac{2(\epsilon_p - \epsilon_h)\langle p|z\tau_z|h\rangle^2}{(\epsilon_p - \epsilon_h)^2 - \omega_d^2} = \frac{-1}{\kappa_D}.$$

For a numerical estimate, we may assume that the single-particle energies are given by the harmonic oscillator spectrum, with

$$\omega_0 = \frac{41}{A^{1/3}} \text{ MeV}.$$

Then the particle–hole excitations are degenerate with $\epsilon_p - \epsilon_h = \omega_0$, and the sum over state can be evaluated with the TRK sum rule. The final result for the dipole frequency ω_D is

$$\omega_D^2 = \omega_0^2 + \frac{3V_\tau}{m\langle r^2\rangle} \approx \frac{75}{A^{1/3}} \text{ MeV}.$$

This is (somewhat fortuitously) close to the empirical frequency in heavy nuclei.

3.4. *Quadrupole motion*

The giant quadrupole mode has a large fraction ($\approx 75\%$) of the sum rule for the pure quadrupolar field

$$S = z^2 - \frac{1}{2}(x^2 + y^2).$$

This field induces irrotational and incompressible flow, and is therefore appropriate for incompressible drops. The velocity field associated with S is

$$\nabla S = (-x, -y, 2z).$$

For spherical nuclei, we may easily evaluate the inertia eq. (3.10) as

$$M_Q = m_N \int d^3r |\nabla S|^2 \rho_0 = 2m_N A\langle r^2\rangle. \tag{3.34}$$

The restoring force coefficient also reduces to a simple expression when the Hamiltonian only has contact interactions. Because the field does not compress the nuclear density, the expectation of a delta function interaction is independent of the deformation. Thus the only part of the Hamiltonian that is affected by the field is the kinetic energy. The operator $\exp(\beta m[H, S])$ makes the following transformation on the coordinates:

$$x \to xe^{-\beta}$$
$$y \to ye^{-\beta}$$
$$z \to ze^{2\beta}$$

The matrix elements of the gradient operator are transformed in the inverse way. The kinetic energy of the deformed wave function becomes

$$\langle\beta|\frac{\nabla^2}{2m}|\beta\rangle. = \langle 0|\frac{\nabla^2}{2m}|0\rangle(e^{2\beta} + e^{2\beta} + e^{-4\beta})/3$$

Expanding this to second order in β, we find the following expression for the restoring force coefficient in eq. (3.11)

$$K_Q = 8\langle 0|\frac{\nabla^2}{2m}|0\rangle \approx \frac{24}{5}A\epsilon_f, \tag{3.35}$$

with ϵ_f the Fermi energy. We can now insert the expressions for the inertia and the restoring force coefficient in the oscillator formula, eq. (3.12). The result is

$$\omega^2 = \frac{12\epsilon_f}{5m\langle r^2\rangle} \approx \frac{65}{A^{1/3}} \text{ MeV}. \tag{3.36}$$

This is close to the empirical value of the giant quadrupole frequency.

Exercise 5: Verify eq. (3.35).

The diabatic quadrupole formula, eq. (3.36), is very interesting in that it does not depend on the interactions at all. The restoring force is strictly an effect of the fermionic nature of the ground state wave function. If we considered a Bose system, the Fermi energy ϵ_f would vanish and there would be no restoring force in the leading approximation. The quadrupolar restoring force is a resistance to shear displacements, a characteristic of solids rather than liquids. Thus the nucleus behaves as a solid at high frequency, with the nodes of the single-particle wave functions providing the memory of shape.

Besides the existence of the giant quadrupole vibration, this shear modulus may also have consequences in heavy ion reactions. In ref. [21], the reaction ^{208}Pb + ^{208}Pb was studied at a bombarding energy of 12 MeV/n, high enough to allow the nuclei to touch and interpenetrate. When they interpenetrate, the stiffness provides a repulsive force that should push the two nuclei apart. Thus, the trajectory of the separation between the two centers would have a sharper turnaround with the diabatic restoring force. This is illustrated in Fig. 3. The electric field in the vicinity of the nuclei would have higher Fourier components as a result, and this would lead to more energetic electric excitations. In

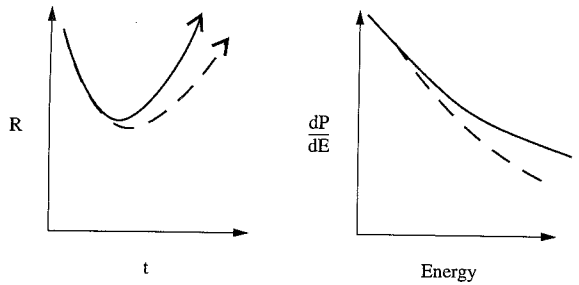

Fig. 3. Graph (a) compares the trajectories of heavy ion collisions in models with (solid) and without (dashed) the diabatic restoring force. Graph (b) compares the spectra of secondary electrons with and without the diabatic restoring force. The measurement in ref. [21] are close to the prediction with the diabatic force included.

fact the experimenters measured the cross section and energy distribution of secondary electrons knocked out of the atoms during the collision process. They found that the rate was higher than the theory without the diabatic force, and it agreed with the theory including the diabatic force. This is also sketched in the figure.

4. Collective motion at low frequencies

The diabatic theory I have presented is only half the story of collective motion. It describes the high-frequency side of the response, but there is considerable collectivity also at low frequency. This may be illustrated with the quadrupole response of the nucleus ^{208}Pb. The transition strengths in the independent particle model and in RPA are shown in Fig. 4. The independent particle model has many transitions in the region of 15–20 MeV that carry most of the strength. With the interaction turned on, the strength is shifted down to two strong peaks. The upper peak may be identified with the diabatic vibration. The lower peak has only 12% of the energy-weighted sum rule, but it has almost the same amplitude as the giant resonance. This part of the strength originates in single-particle transitions that have low transition energy. According to the RPA dispersion relation, the lowest pole of the response is always below the lowest single-particle transition, if the interaction is attractive. This pole is able to gather considerable collective strength, even though the transitions that it is based on are in some sense accidental. Another way to see the collectivity of the low transitions is to measure the radial shape of the transition density. This is shown in Fig. 5 for the quadrupole transition in ^{208}Pb. The collective field eq. (3.4) produces a surface-peaked transition density, and this is very obvious in the measurement. The upper solid line

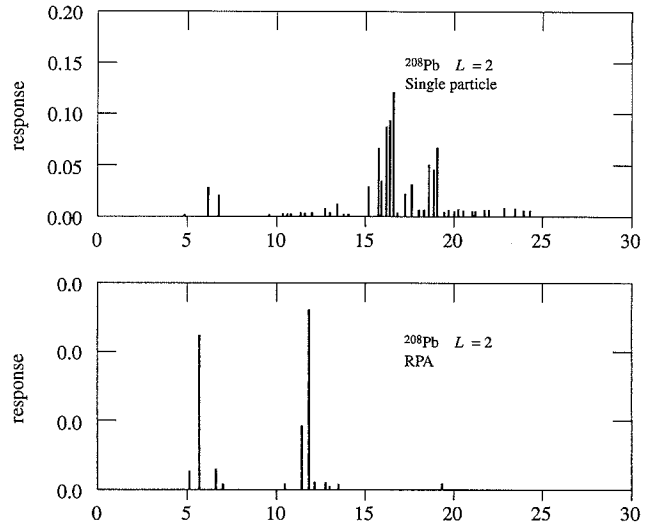

Fig. 4. Quadrupole strength function for ^{208}Pb, from ref. [3]. The upper graph shows the free particle–hole response, and the lower graph shows the RPA.

shows the shape for the pure collective field, eq. (3.4). The lower line shows the RPA prediction of the transitions density. If anything, the empirical shape seems more like the collective flow than the RPA.

4.1. Surface response in the large A limit

A qualitative theory of how the low-frequency response behaves in RPA can be developed in a model treating the nucleus as a semi-infinite slab. I will not go into details of this model; they may be found in ref. [22]. The basic assumption of the model is that the residual interaction can be treated in the separable form, with a surface form factor given by the derivative of the single-particle potential $U_)$. The parameterization is

$$v = \kappa \frac{dU_0}{dz_1}\frac{dU_0}{dz_2}\delta^{(2)}(r_{\perp 1} - r_{\perp 2}).$$

The modes may be characterized by their momentum parallel to the surface $k_\perp$. It may then be shown that the RPA response has an expansion for small ω and $k_\perp$ of the form

$$\Pi^{\mathrm{RPA}} \approx \frac{1}{ia\omega + bk_\perp^2 + \cdots} \tag{4.1}$$

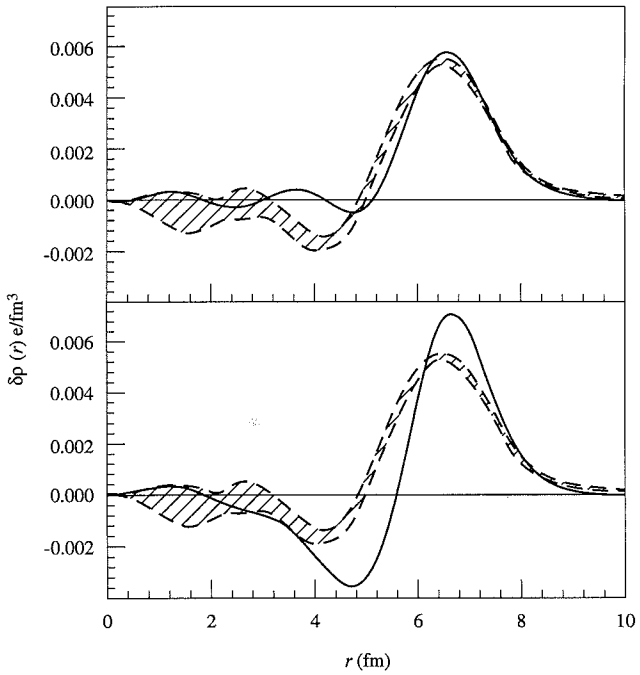

Fig. 5. Transition density for the excitation of the quadrupole state at 4.07 MeV in ^{208}Pb, from ref. [3]. The dashed curves show the experimental data. The upper solid curve is the collective transition density, eq. (3.4), and the lower solid curve is an RPA calculation.

The first thing to notice about this expression is that it diverges as $\omega \to 0$ when $k_\perp = 0$. This is exactly the same phenomenon as gives rise to Goldstone modes in field theory. These arise when there is a degeneracy of the ground state. In the slab model, the position of the surface is indeterminate. We could move the surface and the system would have exactly the same energy. A consequence is that there is a zero-frequency pole in the response for the mode corresponding to a uniform translation of the surface, i.e. $k_\perp = 0$.

The two coefficients in eq. (4.1) have physical interpretations. The coefficient b is proportional to the surface tension, as calculated in mean-field theory. The coefficient a is closely related to the damping constant for collective motion in the "wall formula" for surface dissipation. In fact, the form of the response eq. (4.1) is exactly that of a diffusion equation. A distortion of the surface $z(r_\perp)$ disappears according to the diffusion equation

$$\nabla_\perp^2 z(r_\perp, t) = \frac{a}{b}\partial_t z(r_\perp, t).$$

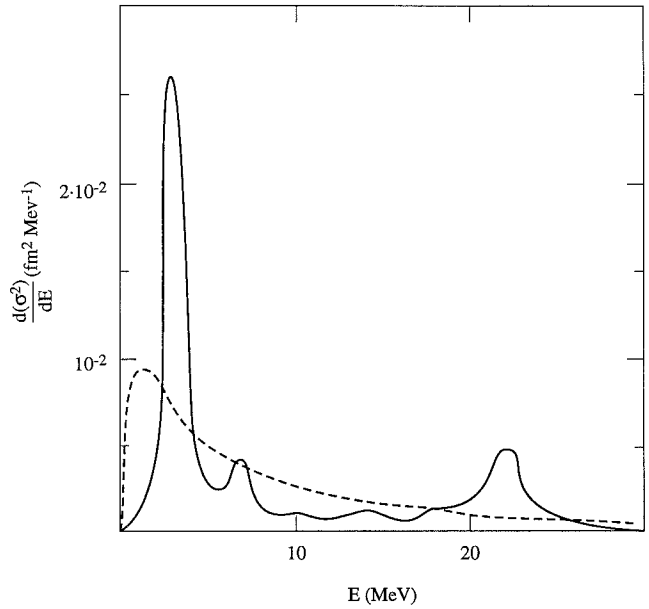

Fig. 6. The slab response (dashed) compared with the RPA octupole response for ^{208}Pb (solid). The ^{208}Pb response has been broadened to allow visual comparison of the areas.

Of course, the shell structure in real nuclei is too pronounced for the slab model to be realistic. Nevertheless, it does describe in some way the average behavior of the RPA response. This is illustrated in Fig. 6, comparing the slab model with the RPA octupole response of ^{208}Pb. The connection between angular momentum L and linear momentum $k_\perp$ was taken as $L = k_\perp R$. The RPA response has a very strong low mode together with a giant octupole at high excitation. The slab model has a single smooth curve with the low energy enhancement.

4.2. *Pairing effects*

In the above paragraph we saw that individual single-particle transitions at low frequency could induce collective behavior. Another mechanism for producing low-frequency collectivity is through the pairing interaction. It is well-known that pairing in a Fermi liquid produces superfluidity. This is nothing more than saying the collective response becomes that of a perfect fluid. As a consequence, with strong pairing the giant quadrupole would disappear at high frequency and be replaced by a low-frequency liquid-drop mode of oscillation.

To see how the pairing works qualitatively, let us look at the gauge description of the pairing wave function introduced in Mottelson's lectures. We consider two kinds of orbitals, and label the total occupancies of the two kinds by N_1 and N_2. The ground state pairing wave function is a superposition over the different values of N,

$$\psi = \sum c(N_1, N_2)|N_1, N_2\rangle$$

Now let us put in a gauge phase ϕ that depends on $N_1 - N_2$,

$$\Psi(\phi) = \sum c(N_1, N_2)e^{i\phi(N_1-N_2)}|N_1, N_2\rangle$$

We will evaluate the expectation of the pairing Hamiltonian with this wave function and we will see that the energy varies with ϕ as $E \sim \phi^2$. Thus the gauge angle ϕ behaves as a momentum, and its coefficient will give the inertia. The pairing energy of a finite system depends on the pairing gap Δ as $E \sim \Delta^2$. Thus the inertia associated with collective motion varies with the pairing gap as $M \sim \Delta^{-2}$.

There are a number of ways the effects of pairing on collective motion can be derived. The most realistic calculations are done with using the generator coordinate method [26]. However, this is rather intransparent despite simplifications which can be made [25]. We can see qualitatively how the pairing works starting from the response function. This is expanded about the adiabatic limit to give eventually the cranking formula (eq. (4.2) below).

The general expression for the response in terms of eigenstates i, f and their energies $E_{i,f}$ is

$$\Pi(\omega) = 2\sum_f \langle i|S|f\rangle^2 \frac{E_n - E_i}{-(E_f - E_i)^2 + \omega^2}.$$

This is expanded to fourth order in ω to give

$$\Pi(\omega) = \sum_n \langle i|S|f\rangle^2 \frac{2}{E_f - E_i} + \omega^2 \sum_n \langle i|S|f\rangle^2 \frac{2}{(E_f - E_i)^3} + \cdots$$

$$= 2M_{-1} + 2\omega^2 M_{-3} + \cdots$$

Now let us make a collective model of the response, in which there is just one transition, to a state $\langle c|$ at a frequency ω_c

$$\Pi(\omega) = \frac{2\omega_c\langle i|S|c\rangle^2}{\omega^2 - \omega_c^2}.$$

We may also expand this in powers of ω. When the two expansions are compared, we find conditions to be satisfied by $\langle i|s|c\rangle$ and ω_c, giving a formula for the collective frequency,

$$\omega_c^2 = \frac{M_{-1}}{M_{-3}}.$$

The response in systems with pairing is conveniently evaluated in the quasiparticle RPA, QRPA. In this framework, the ground state is described by a wave function with BCS pairing. The excitations are quasiparticles; we label a quasiparticle state of orbital i by $|\tilde{i}\rangle$. Then the matrix elements of a local operator are given by

$$\langle 0|S|\tilde{i}\,\tilde{j}\rangle = \langle i|S|j\rangle(u_i v_j + v_i u_j)$$

where u and v are the usual BCS amplitudes. We also need the BCS formula for quasiparticle energies

$$e_{\tilde{i}} = \sqrt{(\epsilon_i - \lambda)^2 + \Delta^2}.$$

Let us now examine the QRPA response function for a separable interaction of the form $\kappa f_1 f_2$. The RPA dispersion relation gives the condition to be satisfied

$$1 - \kappa\Pi^{QP}(\omega_c) = 0$$

where

$$\Pi^{QP} = 2\sum_{ij} \frac{\langle 0|f|\tilde{i}\,\tilde{j}\rangle^2(e_{\tilde{i}} + e_{\tilde{j}})}{\omega^2 - (e_{\tilde{i}} + e_{\tilde{j}})^2}.$$

We expand this equation in powers of ω_c, and solve for the frequency. This yields

$$\omega_c^2 = \frac{1 - 2\kappa\sum_{ij}\langle 0|f|\tilde{i}\,\tilde{j}\rangle^2/(e_{\tilde{i}} + e)}{2\kappa\sum_{ij}\langle 0|f|\tilde{i}\,\tilde{j}\rangle^2}/(e_{\tilde{i}} + e_{\tilde{j}})^3.$$

The numerator, when multiplied by κ, is the restoring force constant for the field f. The denominator must then be the inertia. The result is very similar to the cranking inertia, and with some manipulation can be expressed in that form.

To make the connection, we first note that the mean field Hamiltonian is $H = H_0 + \kappa f\langle f\rangle$, so $\kappa f = dH/d\langle f\rangle$. Second, we note that the most important transitions in Π^{QP} will be diagonal ones with $i = j$. Then we may write the inertia as

$$M = 2\kappa^2 \sum_i \frac{\langle 0|f|\tilde{i}\tilde{i}\rangle^2}{(2e_{\tilde{i}})^3} \approx \sum_i \langle i|\frac{dH}{d\langle f\rangle}|i\rangle^2 \frac{u_i v_i}{e_{\tilde{i}}^3}. \tag{4.2}$$

This is called the cranking formula for the inertia [27]. Now if we replace the sum by an integral over states, we can easily extract the Δ-dependence. The factor $u_i v_i$ is nonzero in an energy interval of the order of Δ. The integration thus produces

a factor of Δ, reduced to Δ^{-2} by the factor $e_{\tilde{i}}^{-3}$ in the integrand. Thus we find the adiabatic inertia from pairing scales as

$$M \sim \frac{1}{\Delta^2}.$$

When one puts in numbers for the quadrupolar inertia appropriate to heavy nuclei, the adiabatic inertia comes out about ten times the diabatic (or irrotational) inertia. The diabatic inertia increases with A as $A^{5/3}$. The adiabatic inertia increases more slowly with A. If we assume that the pairing gap is independent of A, the cranking formula (4.2) has only a linear increase with A, due to the sum over particles. The two inertias would become equal at some point, and this would mark the transition to superfluid dynamics. From the numbers, this point would be for A in the ten thousands, far beyond the stability limits for physical nuclei.

5. Nuclear equation of state

Nuclear matter is an abstraction that theorists like to think about. The starting points are the semiempirical mass formula, whose leading term is a binding energy of about 16 MeV per nucleon, and the measured nuclear radii, whose $A^{1/3}$ scaling implies a saturation of nuclear matter with an interior density of about $\rho_0 = 0.16$ nucleons/fm^3. Since the early 1960's theorists sought to explain these two properties of nuclear matter taking as their starting point empirical knowledge of the nucleon–nucleon interaction. One immediate problem with this program is that "the" nucleon–nucleon interaction is not known. One can measure nucleon–nucleon scattering phase shifts accurately (see http://nn-online.sci.kun.nl for recent fits), but phase shifts by themselves are not sufficient to determine an interaction. If one assumes in addition that the potential is local, one has sufficient constraints to construct fairly unambiguous potentials. These potentials showed that nuclear matter was a more difficult problem than had been suspected: predictions were either grossly underbound or overdense or both. The reasons for the failure could lie in the following areas:

- neglected relativity
- missing subnucleon degrees of freedom
- three-body forces.

The last possibility is just a phenomenological way to treat missing degrees of freedom, since all the forces very likely arise from QCD with its quarks and gluons.

This history has serious implications for the theory of finite nuclei. Namely, we cannot expect to start from a realistic Hamiltonian and reliably derive properties of actual nuclei. We are stuck treating the Hamiltonian phenomenologically until the nuclear matter problem is put to rest. In some way this makes theory easier. Freed from the edict, "Thou shalt use this Hamiltonian", one can invoke approximations that simplify the problem at hand. We saw examples of this in the sections on collective motion.

Let us proceed in a similar spirit for nuclear matter. We need to start with some many-body theory. Our organizing principle will be that nuclear matter can be described as a moderately dilute Fermi gas, so we may expand the energy in powers of the density*. Details can be found in books on many-body quantum mechanics, for example, [28]. The first term in the expansion is the Fermi gas kinetic energy. This contributes to the energy per particle an amount $E_1 = 3k_f^2/10m_N$. It scales with number density n as

$$E_1 \sim n^{2/3}. \tag{5.1}$$

The next term is the two-body interaction energy. Its contribution to the energy per particle may be written as

$$E_2 = vn \tag{5.2}$$

where v is a constant with dimensions of energy-length^3. We can now begin to make a theory of nuclear matter using the density n as an expansion parameter.

The two terms we have discussed are insufficient to make a theory of nuclear saturation. The second term must be attractive to bind nuclei, but it increases more rapidly with density than the first term, so the predicted nuclear matter would be infinitely dense. We need at least one more term in the series. Naively, one might expect the next term to be a three-body interaction. This would giving an energy per particle having one higher power of n than eq. (5.2) for the two-particle interaction. In fact the n-dependence of the next term in the expansion is different. The reason is that the effective interaction is modified by the Pauli principle, which in effect makes $k_f \sim n^{1/3}$ the expansion parameter in a power series. The first two terms vary as k_f^2 and k_f^3, respectively. To see dependence of the next term, let us define an effective interaction at zero density, with a matrix element t between plane–wave states. At finite density, the interaction is weakened by Pauli blocking of intermediate states. Perturbatively, one obtains the energy shift ΔE of the interaction between two particles from the integral

$$\Delta E_2 = \int_{\text{occupied}} d^3k \quad t\frac{1}{\epsilon(k)}t. \tag{5.3}$$

Note that the integral over occupied states scales with k_f as k_f^3, but the energy denominator also increases with k_f, going as k_f^2. Thus the correction to the pair

* Actually, the low-density expansion is only well defined if a zero-density limit exists. That may not be the case for attractive potentials: if finite self-bound clusters exist, then the low-density limit will be a gas of clusters, not of free particles. But I will ignore this question of principle.

energy varies as k_f. The energy per particle is proportional to the density times the correction, k_f^4. Thus the next term in the series varies as $n^{4/3}$.

With these considerations, the simplest phenomenological model we can construct that has the saturation property is the three-term formula,

$$E_0(n) = \frac{3}{10}\frac{k_f^2}{m} + v_a n + v_b n^{4/3}. \tag{5.4}$$

It is convenient to use units in which the density n is one at nuclear matter density, $\rho = n\rho_0$. Then nuclear matter properties are fit with parameter values

$$\begin{aligned} v_a &= -107.2\ \text{MeV}, \\ v_b &= 69.6\ \text{MeV}. \end{aligned} \tag{5.5}$$

By construction, eq. (5.4) has a minimum at $n = 1$ and $E(1) = -16$ MeV. As mentioned in a footnote, the region $n < 1$ is in some sense unphysical because nuclear matter at lower density would break up into separated nuclei. However, the region slightly below $n = 1$ might be reachable in the dynamics of heavy ion collisions, and might be metastable with respect to fragmentation.

Next let us calculate the equation of state (EOS). The EOS is the pressure expressed as a function of density and temperature. The pressure may be defined as the adiabatic energy derivative,

$$P = -\left.\frac{\partial EA}{\partial V}\right|_S = \rho_0 n^2 \left.\frac{\partial E}{\partial n}\right|_S. \tag{5.6}$$

The derivative is easy to evaluate out at zero temperature, because the entropy is then constant. Carrying this out for eq. (5.4), we find

$$P = \frac{2}{5} e_f \rho_0 n^{5/3} + v_a \rho_0 n^2 + \frac{4}{3} v_b \rho_0 n^{7/3}. \tag{5.7}$$

This EOS is sketched in Fig. 7. We see that the pressure vanishes in equilibrium ($n = 1$), as it must, and that it is negative in the unphysical region.

The derivative of the pressure gives the compressibility of nuclear matter. This is defined as

$$k = n\frac{dP}{dn}. \tag{5.8}$$

Conventionally in nuclear physics this is expressed as the incompressibility coefficient K

$$K = 9\frac{k}{n} = 9\frac{dP}{dn}. \tag{5.9}$$

The above EOS gives a compression modulus of $K = 235$ MeV. We will see shortly that this is somewhat higher than what is required to fit the giant monopole vibration.

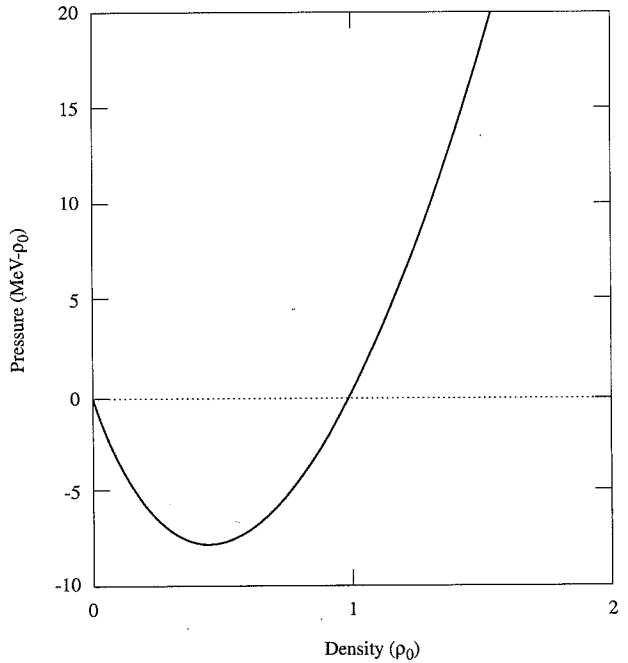

Fig. 7. The nuclear matter energy function, eq. (5.7).

5.1. Finite excitation energy

Let us now consider nuclear matter at a finite temperature. We shall assume that the thermal energy goes entirely into particle kinetic energy, not affecting the interaction energy. This will simplify the discussion considerably. To calculate the thermal properties, we need the relation between excitation energy per particle ϵ, entropy per particle s, and temperature T. In the Fermi gas model at low temperature, the excitation energy per particle is given by

$$E_{\text{ex}} = \frac{\pi^2}{4}\frac{T^2}{e_f}, \quad \text{for } T \ll e_f \tag{5.10}$$

On the other hand, at high temperature the system behaves as a classical gas, with a relation

$$E_{\text{ex}} = \frac{3}{2}T \quad \text{for } T \gg e_f \tag{5.11}$$

A function that interpolates between these two limits and is accurate to a few tenths of a percent in between is

$$E_{\rm ex}/e_f = -0.3 + \sqrt{0.09 + t^2\left(2.25 - \frac{0.7697}{1+t}\right)} \tag{5.12}$$

where $t = T/e_f n^{2/3}$ is a dimensionless scaled temperature.

The entropy per particle is a dimensionless quantity, and in the Fermi gas model can only depend on the combination of variables $T/e_f \sim T/n^{2/3}$. This makes it quite easy to find adiabatic derivatives. The pressure at finite entropy density is given by

$$P = \left.\frac{dE}{dn}\right|_T - \left.\frac{dE}{dT}\right|_n \left.\frac{dT}{dn}\right|_S \tag{5.13}$$

$$= \left.\frac{dE}{dn}\right|_T - \left.\frac{2T}{3n}\frac{dE}{dT}\right|_n$$

where $E = E_0 + E_{\rm ex}$. The pressure curve for a range of entropies is shown in Fig. 8.

We see that the EOS is similar to the classical Van der Waals EOS, with coexisting phases when the temperature is not too high. This is the theoretical gas–liquid phase transition of nuclear matter. There is a critical point at $T \approx 18$ MeV. Campi's lectures discuss the physics of finite nuclei in this region.

Exercise 6: Find the critical temperature numerically, using eq. (5.7) and eq. (5.12).

5.1.1. Compressibility and the monopole resonance

The giant monopole resonance is the specific observable in nuclear spectroscopy that relates to the compressibility of nuclear matter. If nuclei could be treated as sharp-edged spheres, the compressibility could be determined directly from the response to the field

$$S = r^2/2. \tag{5.14}$$

The inertia may be calculated from eq. (3.10) and is

$$M = Am_N\langle r^2\rangle. \tag{5.15}$$

The restoring force coefficient, using the nuclear energy function eq. (5.4), is given by

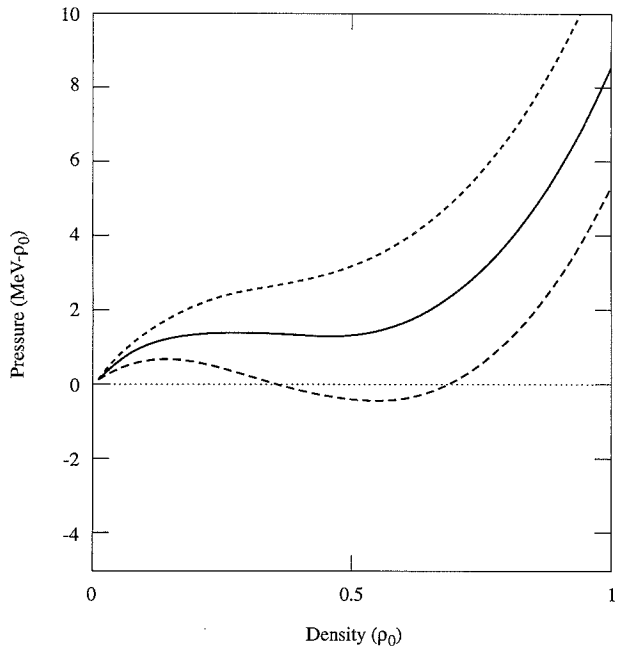

Fig. 8. Pressure at finite excitation energy, from eqs. 5.7 and 5.13. The different plots are at constant entropy, corresponding to the following temperatures at $n = 1$: 12 MeV (long dashed); 18 MeV (solid); 20 MeV (short dashed).

$$K = \partial_\beta^2 \langle\psi_\beta|H|\psi_\beta\rangle|_{\beta=0} =$$

$$\rho_0\left[4\int d^3r\,\tau_0(r) + 9v_a\int d^3r\,n_0^2(r) + 16v_b\int d^3r\,n_0^{7/3}(r)\right]. \tag{5.16}$$

This is exactly A times the nuclear matter incompressibility coefficient K, if one can make the large-A approximations $n(r) = \theta(R-r)$, $\tau_0(r) = 3e_f\theta(R-r)/5$ to evaluate the integrals. In this limit, the formula for the monopole frequency is

$$\omega_M^2 = \frac{K}{M} = \frac{K_\infty}{m_N\langle r^2\rangle}. \tag{5.17}$$

To get a value for the incompressibility coefficient K_∞, we recall that the empirical frequency is given by

$$\omega_M \approx 80/A^{1/3}\ \text{MeV}. \tag{5.18}$$

The eq. (5.17) has this A-dependence, and the coefficient 80 MeV is obtained if one takes $K_\infty = 133$ MeV and $\langle r^2 \rangle = 3(1.2 \text{ fm})^2 A^{2/3}/5$. Unfortunately, surface effects spoil the approximation leading to eq. (5.17). The fact of the matter is that the surface has an exaggerated importance because the v_a and v_b are separately large with opposite signs. For quantitative purposes, it is necessary to start from specific mean field models, and calculate the RPA frequencies of the monopole for the models. This has been done by Blaizot and collaborators [29,30]. They found that there is a close connection between compressibility and the monopole frequency, with the surface effectively lowering K in eq. (5.17). We can see how this works by looking at the integrals in eq. (5.16) more carefully. Let us parameterize the density with a finite surface by the Fermi function, $n = 1/(1 + \exp((r - R)/a)$. Then the integrals in eq. (5.16) have the expansion

$$\int d^3 r n^k(r) = \frac{4\pi R^3}{3}(1 + \frac{c_k a}{R} + \cdots).$$

The spring constant is then altered to

$$K_A = K_\infty + (9c_2 v_a + 16 c_{7/3} v_b)\frac{a}{R} \tag{5.19}$$

$$\approx 235 - 920\frac{a}{R} \text{ MeV}.$$

In the last step we evaluated the correction numerically using eq. (5.7). Note the very large coefficient of a/R in the above equation. Even for a nucleus as large as ^{208}Pb, the correction is large, of the order of 70 MeV. Thus the empirical monopole frequency implies a nuclear matter incompressibility of the order $K_\infty \approx 133 + 70 \approx 200$ MeV.

Another question we need to ask is how well the radial compressional field eq. (5.14) describes the monopole. No empirical information can be obtained about this, because the only way the monopole has been clearly seen is with hadronic reactions that are dominated by the surface displacement, and are insensitive to the motion in the interior. However, we may again go to the RPA calculations and see what they predict for the collective mode. In the hydrodynamic radial oscillation of a uniform sphere, the surface is free and the compression is reduced near it. This implies that the field S is not so steep at the surface as implied by eq. (5.14). However, with usual mean field models, the incompressibility is also reduced in the surface, allowing S to be steeper there. The two effects compensate and the theoretical velocity field for the RPA mode [29,30] is quite close to eq. (5.14).

One final point that should be mentioned is that RPA calculations with relativistic mean field models do not fit in the overall systematics [36]. In my view, this is related to the difficulty in separating the Dirac sea from the valence particles in the relativistic dynamics. The sum rules are certainly more obscure in the relativistic models because of the negative energy states.

6. Damping of collective motion

Of the three parameters that describe vibrations — the strength, the frequency, and the damping rate, the last is the hardest to calculate. At that stage, one must understand all the degrees of freedom that can couple to the vibration. Not only the coupling strength, but the density of states of these degrees of freedom is important. A systematic procedure is to employ Fermi's Golden Rule, which is equivalent to evaluating the self-energy in second-order perturbation theory.

When I discussed collective motion in Section 3, there was just a single degree of freedom β together with its associated velocity α. In TDHF one has of course the full set of dynamic variables associated with A independent single-particle wave functions. Thus TDHF will automatically introduce damping mechanisms, as the coherence between the motion of different particles dissipates. This dissipation mechanism was first discussed by Landau in the context of classical plasmas, and it is commonly called Landau damping in the context of Fermi liquids as well. The coherence of the collective excitation also disappears when particles escape the nucleus. TDHF with a proper description of the continuum of unbound states includes this damping as well. Finally, there are the damping mechanisms beyond mean field theory, such as mixing with multiple particle–hole excitations. These are in fact the most important and the poorest understood in the nuclear giant resonances.

6.1. Landau damping

Collective frequencies ω_c are determined largely by the interaction in the Hamiltonian. When these are degenerate with a large number of single-particle excitations ($\omega = \epsilon_p - \epsilon_h$), the mixing produces Landau damping. In nuclear physics, shell effects are crucial in determining the level density of single-particle excitations, and each multipole has to be examined individually. We shall do so in a little bit, but first let me tell you about a system where the theory simplifies enormously.

This is the damping of the Mie resonance in atomic clusters. The Landau damping mechanism was studied by Kawabata and Kuba. Their formula may be derived by treating the fluctuating potential field in the Mie resonance as a perturbation in Fermi's Golden Rule, connecting the resonance to single-particle

excitations [3]. Their result is remarkably simple. The width is given by

$$\Gamma = \hbar \frac{v_f}{R} \tag{6.1}$$

where v_f is the Fermi velocity and R is the radius of the atomic cluster. The physics is very simple in this formula: the particles lose coherence when they hit the wall of their container.

If one applies this formula to nuclei or to small atomic clusters (N $\leq$ 500), one gets much too large a damping rate. As an example, take the nucleus ^{16}O. The Fermi velocity is about $v_f \approx 0.3$ c, and the ^{16}O radius is R $\approx$ 3 fm. This gives $\Gamma \sim 20$ MeV, of which would make the giant dipole at a frequency of $w_c \approx 25$ MeV too broad a resonance.

The way the shell effects come in may be seen from the harmonic oscillator spectrum, which is a first approximation to single particle Hamiltonian for N $\leq$ 100. Calling the oscillator frequency ω_0, the single-particle excitations are at frequencies $n\omega_0$, with odd n for odd parity excitations such as the giant dipole, and even n for even parity excitations, such as the monopole and quadrupole. Thus there are gaps of size $2\omega_0$ in the single-particle excitations for any given multipole. If the collective frequency is in the gap region, it will not mix strongly, and can be seen in the TDHF as a single resonance.

This turns out to be the qualitative behavior of TDHF for dipole excitations in light nuclei: the resonant frequency is at $\sim 2\omega_0$ which is a gap region for odd particles. In heavy nuclei, the spin-orbit splittings of the single particle states spoils the simplicity of the harmonic oscillator picture, and there is predicted to be considerable Landau damping. This is illustrated in Fig. 9 which shows the RPA spectrum of the giant dipole in ^{208}Pb. The individual peaks may be associated with single-particle excitations at nearby frequencies. The experimental strength function is quite different: it is single broad and smooth peak, well fit by the Lorentzian function. Obviously, there is important physics beyond RPA when damping is to be calculated.

The RPA is more successful in the nucleus ^{16}O. The photon cross section for this nucleus is shown in Fig. 10. The main strength is split into two peaks. RPA reproduces this, as a mixing between collective resonance and the single-particle excitation $(p_{3/2}^{-1} d_{3/2})$, which has a high frequency because of the spin-orbit field.

6.2. *Direct escape*

There is a second source of damping in TDHF, associated with the particles in the continuum leaving the nucleus. The particle escape in TDHF should be distinguished from the evaporation of particles that may occur after the vibrational motion has been dissipated into other degrees of freedom.

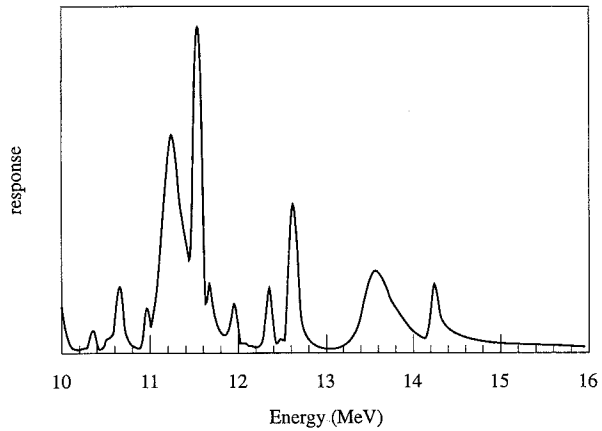

Fig. 9. The giant dipole resonance in ^{208}Pb according to RPA, from ref. [3].

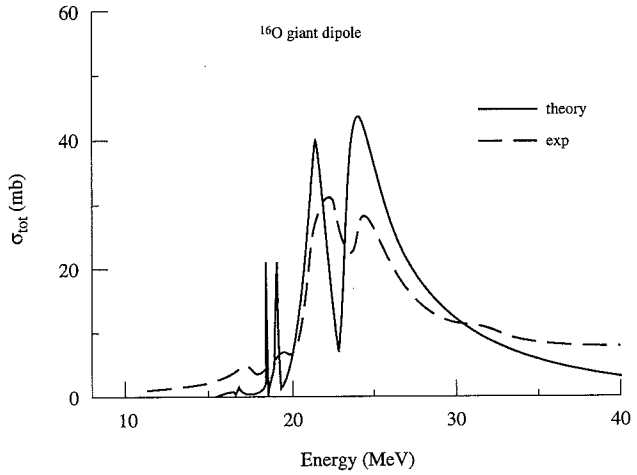

Fig. 10. The giant dipole resonance in ^{16}O, from ref. [3]. The experimental photoabsorption cross section is shown as the dashed line, and an RPA calculation is shown as the solid line.

Before displaying the RPA results, it is helpful to estimate the width from more elementary arguments. Let us start with the idealization of free particles in a spherical volume. The rate at which particles cross the surface of the volume will be the damping rate associated with escape. The classical calculation is given

by the integral below

$$W = n\pi R^2 \int_0^{4\pi} \frac{d\phi}{4\pi} \int_0^1 d\cos\theta\, v\, \cos\theta \tag{6.2}$$

$$= \frac{3}{4}\frac{v}{R}.$$

In the above equation, $n = 3/4\pi R^3$ is the number density, R is the radius of the sphere, and v is the velocity of the particle. The angular integral is over the direction of the particle with respect to the normal of the surface. The above estimate is far too naive because it ignores the potential well that holds the particles in and slows them down as they leave. We can improve on eq. (6.2) by explicitly putting in the potential barrier physics. We consider a barrier of height U_0, and take a particle that has enough energy to escape, with $E = U_0 + \epsilon$. We will assume that the particle escapes from the potential if the kinetic energy associated with the radial motion exceeds the barrier. Labeling the direction of motion of the particle with respect to the wall by the angle θ, we need the following integral to get the flux of particles over the barrier,

$$\int_{\theta_0}^1 d\cos\theta \sqrt{\frac{2(U_0+\epsilon)}{m}} \cos\theta = \frac{1}{2}\sqrt{\frac{2}{m(U_0+\epsilon)}}$$

where $\theta_0 = \cos^{-1}\sqrt{U_0/U_0+\epsilon}$ is the angle at which the radial momentum is just large enough to surmount the barrier. The formula for the width is then

$$\Gamma = \frac{3\epsilon}{4R}\sqrt{\frac{2}{m(U_0+\epsilon)}}. \tag{6.3}$$

Let us see how this works in practice, taking as a first example the nucleus ^{16}O. The GDR is centered at about 25 MeV. Since the Fermi level at -16 MeV and the well depth is about $U_0 = 50$ MeV, escaped particle has a kinetic energy $\epsilon \approx 9$ MeV. Using $R = 3$ fm for the radius of ^{16}O, the formula gives a width of 3 MeV. Looking back at Fig. 9, we see that this is the approximate width of the main peak. Thus the escape width is quite important for the giant resonance in ^{16}O.

Next let us examine a heavy nucleus, ^{208}Pb. The corresponding numbers to put in eq. (6.3) are $\epsilon \approx 4$ MeV, $U_0 \approx 44$ MeV, and $R \approx 7$ fm. This applies to the neutron decay channels. The proton channels are effectively closed due to the large Coulomb barrier, reducing the width by an additional factor of Z/A. The formula then gives a width of ~ 0.2 MeV. Looking back at Fig. 8, we see that the individual peaks are quite narrow. Their total width is not far from the value given by the the formula. However, as mentioned before, the experimental strength function looks nothing like the RPA theory: it is a single smooth peak

just like the lower curve in Fig. 1. We conclude that the escape width in heavy nuclei is small compared to the damping due to mechanisms beyond RPA. Those form the topic of the section below.

6.3. *Beyond mean field*

As we saw earlier, it is necessary to go beyond mean field theory to treat the damping in heavy nuclei. Many-body theory provides a systematic procedure for mixing other degrees of freedom, treating them as multiparticle–multihole states. The collective excitation is a superposition of one-particle–one-hole states, and it mixes with two-particle–two-hole states by the residual interaction. As a first approximation which is very useful for an orientation, let us consider the coupling to the particle and the hole of the collective excitation to be incoherent. We then have the width expressed in terms of a particle and hole decay widths as

$$\Gamma_{ph}(\varepsilon_{ph}) = \Gamma_p(\varepsilon_p) + \Gamma_h(\varepsilon_h). \tag{6.4}$$

We have explicitly indicated that the width depends on excitation energy. Let us for the moment assume that this formula is valid, and ask about the origin and magnitude of the single-particle damping widths, $\Gamma_p(\epsilon)$ and $\Gamma_h(\epsilon)$. According to the Golden Rule formula,

$$\Gamma_p(\epsilon) = \overline{\langle p|v|p'\,p''\,h''\rangle^2} \int dn_{p'} dn_{p''}\, dn_{n''} \delta(\epsilon - (\varepsilon_{p'} + \varepsilon_{p''} - \varepsilon_{n''})). \tag{6.5}$$

The second factor is the density of 2p–1h states. It is responsible for the dependence of the width on energy E, for energies in the vicinity of the Fermi surface.

The two-particle–one-hole density of states is proportional to $(\epsilon - \epsilon_f)^2$, which may be seen quite easily as follows. We start with the single-particle density of states n_ϵ and build up the multiparticle density of states by convolution. We may take n_ϵ as constant near the Fermi surface; in the Fermi gas model it is given by

$$n_\epsilon = V \int \frac{d^3k}{(2\pi)^3} \delta(\epsilon - \epsilon_k) = \frac{3}{2}\frac{A}{E_F}\left(\frac{\epsilon}{e_f}\right)^{1/3} \tag{6.6}$$

$$\approx \frac{3}{2}\frac{A}{E_F}, \quad \text{for } \epsilon \approx \epsilon_f. \tag{6.7}$$

The one-particle–one-hole density of states is just the convolution of one particle densities,

$$\int dn_p dn_h\, \delta(\epsilon - (\epsilon_p - \epsilon_h)) = n_\epsilon^2 \int_{\epsilon_f} d\epsilon_p \int^{\epsilon_f} d\epsilon_h\, \delta(\epsilon - (\epsilon_p + \epsilon_h))$$

$$= n_\epsilon \epsilon. \tag{6.8}$$

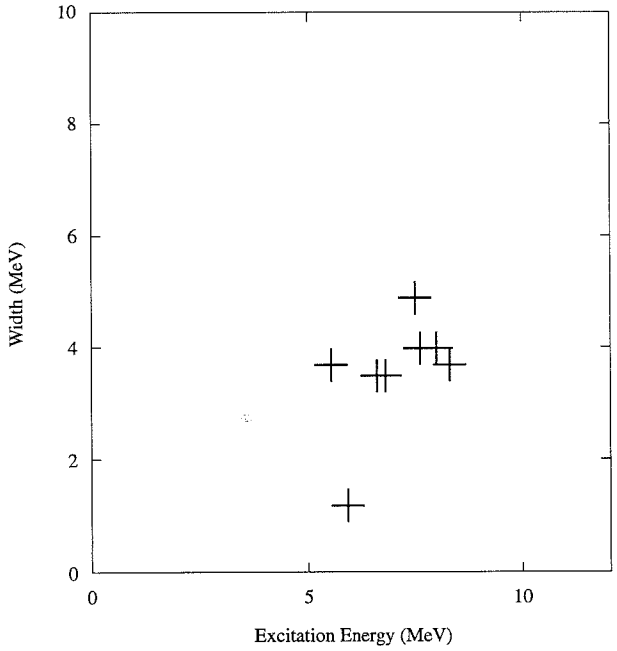

Fig. 11. Widths of single-particle states, from the table in ref. [37], as a function of energy.

Note that this depends linearly on the energy ϵ. A second convolution gives the 2p–1h density of states,

$$\int dn_p\, dn_{p'}\, dn_{h'}\, \delta(\epsilon - (\varepsilon_p + \varepsilon_{p'} - \varepsilon_{h'})) \tag{6.9}$$

$$= n_e^3 \frac{(\epsilon - \epsilon_f)^2}{2}. \tag{6.10}$$

Thus the Fermi gas model predicts that the single-widths have the leading behavior

$$\Gamma_{p,h} = a(\epsilon_{p,h} - \epsilon_f)^2 \tag{6.11}$$

in the vicinity of the Fermi surface. There have been attempts in the literature to parameterize the single-particle widths using functions with this leading behavior. See ref. [37] for some examples. Experimentally, the single-particle width can be studied with particle-transfer reactions. A graph of the data is shown in Fig. 11. A glance at it should convince the reader that there is not sufficient regularity to make a simple parameterization such as eq. (6.11) reliable. However, there are many cases where the width is about 3–4 MeV when the excitation away from

the Fermi surface is ~8 MeV. These numbers correspond to $a \sim 1/20$ MeV in eq. (6.11), and that is a value that has often been used.

Part of the difficulty with the parameterization eq. (6.11) is that the Fermi gas model ignores the collective physics associated with the surface. We saw earlier that there is strong surface collectivity that couples to the single-particle motion. We can make a very qualitative argument about how the surface collectivity behaves using the slab model. The final state density can be expressed as a single-particle level density multiplied by the imaginary part of the particle-hole response. Taking the response from eq. (4.1), the integral is

$$\Gamma(\epsilon) \sim \mathrm{Im} \int_0^\epsilon d\omega \int_0^\Lambda d^2k_\perp^2 \frac{1}{i\omega + bk_\perp^2/a},$$

where Λ is a cutoff having the order of magnitude of the Fermi momentum.

The integral over $k_\perp^2$ is obviously a logarithm, $\ln(\Lambda^2 + i\omega b/a) - \ln(ia\omega/b)$. The imaginary part of $\log(ia\omega/b)$ is a constant, $i\pi/2$, so the integral over ω just gives a linear dependence on ϵ. Of course, the slab model is grossly oversimplified, and the final message might be that the width on average should depend on excitation energy as a power E^α with $1 < \alpha < 2$.

Let us now return to the giant resonances, and consider as an example a collective excitation at an energy of 16 MeV. Splitting the energy equally between particle and hole, the damping width would be

$$\Gamma_{ph}(16\ \mathrm{MeV}) \sim 2\,\Gamma_p(8\ \mathrm{MeV}) \sim 6 - 8\ \mathrm{MeV}. \tag{6.12}$$

The collective resonances are in fact narrower than this. The reason is that there is a coherence between particle and hole, which interferes destructively in the matrix element to create a secondary particle–hole pair [37]. We could calculate this again by using Fermi's Golden rule. The matrix element would be the sum of the particle and hole contributions,

$$\langle ph|v|p'\,p''\,h''\,h'\rangle = \langle p|v|p'\,p''\,h''\rangle\delta_{hh'} + \langle h|v|p''\,h''\,h'\rangle\delta_{pp'}. \tag{6.13}$$

When the matrix element is squared, the cross term gives a destructive interference. The physics here is exactly the same as you have heard in a different context: the color transparency discussed by Pire in his lectures. Here the collective state is a quark–antiquark pair that propagates through hadronic matter. The matrix element to excite the matter by the gluon field is reduced because of the interference between quark and antiquark.

7. Large amplitude motion

Under this heading, I want to talk about two unrelated topics. The first is collective motion beyond the harmonic approximation. This is studied experimentally by

creating multiple phonons and measuring their interactions and energy shifts. The other topic in large amplitude motion relates to P. Paul's lectures on fission. The shape change of a nucleus undergoing fission is the largest amplitude motion we can possible study. It is not collective, however, and so quite different theoretical considerations are required.

7.1. Multiple phonons

Since the early days of nuclear physics, collective motion has been treated modeling the Hamiltonian with a harmonic oscillator acting on some intrinsic coordinate. So it is not surprising that extensive searches have been made for the higher excitations of the harmonic oscillator. A famous but deceptive example is the low excitation spectrum of the nucleus ^{112}Cd. The nucleus possesses a 2^+ first excited state at 0.62 MeV excitation energy, and then a triplet of levels at nearly double the energy having quantum numbers 0^+, 2^+ and 4^+. It was natural to think that these states were just double excitations of a nearly harmonic vibration. However, later work showed contradictions in this simple picture. For example, the lowest 2^+ has a substantial quadrupole moment, which is not allowed for a harmonic vibration. The B(E2) transition strengths from the upper levels also do not have the proper relation to the lowest B(E2) to identify them as states of a common harmonic oscillator*. In recent years, experiments have concentrated on the 3^- vibration in ^{208}Pb as a good candidate for a harmonic vibrator. Very recently, evidence for the double 3^- with total angular momentum 0, $(3^- \times 3^-)^0$, was found [32]. In this work, the excitation energy was found to differ from the harmonic value of 2 E_{3^-} by only 0.2%. It is a theoretical challenge that we will not address to try to understand these low collective states.

Recently it has become possible to observe a double excitation of the giant dipole resonance [33–35]. The diabatic collective excitations are much easier to deal with theoretically, because the excitation operator is simple. As we saw in Section 3.1, the collective motion can then be described by the coordinate β, which satisfies equations of motion that can be expressed in terms of integrals over the wave function. It appears that the nonlinearity can then be attributed largely to the behavior of the integral $\langle\beta|H|\beta\rangle$, which we treated earlier in a purely harmonic approximation. I do not wish to go into lengthy calculations of the nonlinearity, but would rather just examine orders of magnitude in the nonlinear behavior†.

For all the modes we have considered, the nonlinearity appears as a small parameter, namely the amplitude of the displacement divided by the nuclear radius.

* See, however, ref. [31] for a more extensive spectrum of ^{112}Cd showing a very regular behavior of the yrast spectrum, 0^+, 2^+, ..., 12^+.

† Ref. [17] has a detailed discussion of the nonlinear theory.

Before demonstrating that this is the relevant parameter for anharmonicity, let us just confirm that it is indeed a small quantity. For the giant quadrupole resonance, we could argue as follows. In terms of the coordinate β, the amplitude of the harmonic motion at an energy $E = \omega/2 = \frac{1}{2}\sqrt{K_Q/M_Q}$ is given by

$$\beta_0 = \frac{1}{(M_Q K_Q)^{1/4}} \tag{7.1}$$

where the inertia M_Q and the spring constant K_Q were defined in Section 3.4. From eq. (3.34) and eq. (3.35) we find

$$\beta_0 = \left(\frac{5}{48 e_f m_N \langle r^2\rangle A^2}\right)^{1/4}. \tag{7.2}$$

This is easily seen to vary with A as $A^{-2/3}$, which goes to zero in the large-A limit. For example, putting in numbers for the physical quantities the amplitude has a value $\beta_0 \simeq 0.015$ for ^{208}Pb, which is indeed much less than 1.

Let us now see how the anharmonicity affects the frequency. There are several ways to calculate this. Perhaps the easiest is to just consider the anharmonic terms in the Hamiltonian as a perturbation on the harmonic oscillator states. Thus, if we write the energy function as

$$\langle\beta|H|\beta\rangle = E_o + \frac{1}{2}K_Q\beta^2 + \frac{1}{4}K'_Q\beta^4 + \ldots \tag{7.3}$$

we may estimate the energy shift as

$$\Delta E_n = \frac{1}{4}K'_Q \langle n|\beta^4|n\rangle. \tag{7.4}$$

To derive the A-dependence of this expression, note first that the expectation of the Hamiltonian scales as A. Since the coordinate β is dimensionless, this implies that the integrals defining the coefficients K and K'_Q also scale as A. Putting this and the $\beta \sim A^{-2/3}$ scaling into the above equation we find $\Delta E_n \sim A^{-5/3}$, This is a factor $A^{-4/3}$ faster than the basic quadrupole frequency, $\omega \sim A^{-1/3}$. This simple argument is confirmed by more detailed calculation [17].

It is interesting to put this in the context of a general many-particle system with collective excitations, for example phonons or plasmons. A phenomenological Hamiltonian would allow these modes to be coupled with a contact interaction. This would imply frequency shifts that for double excitations that would vary inversely with the volume. Thus it is quite natural to expect an A^{-1} behavior of the anharmonicity in a system of A particles.

Turning back to the nuclear excitations, let us now consider the dipole mode which is of especial interest in view of the experiments [33–35]. To analyze that case, I will treat the mode in the Steinwedel–Jensen model. The displacement

field eq. (3.20) produces a density change (with neutrons opposite to protons) in the interior but not in the surface. The collective coordinate β has in this case dimensions of length squared; the associated displacement field is proportional to $k^2 \sim 1/R^2$. Let us now see how the amplitude of the vibration depends on size using the formula $\beta_0 = (M_D K_D)^{-1/4}$. The mass and restoring force constants in eq. (3.22) and eq. (3.23) scale with A as

$$M_D \sim A^{1/3}$$
$$K_D \sim A^{-1/3},$$

implying that β_0 is independent of A. For a given β_0, the energy function varies with A as A times the appropriate power of k, giving an $A^{-2/3}$ dependence for the quartic term. Thus the small anharmonicity for large nuclei is also a characteristic of the dipole mode. The result is also similar assuming that the mode is of the Goldhaber–Teller type. In detailed numerical models, the second dipole is within a small fraction of an MeV of being at twice the single resonance frequency. On the experimental side, the double excitation was found to be at the expected energy.

However, some experimenters reported a strength for the second excitation significantly larger than expected from harmonic theory. The collective state satisfies a sum rule, and there is no way to alter its strength with shifting its frequency correspondingly. A likely explanation of the experimental results is that other multipolarities in the same region of the spectrum contributed to the observed bump.

I want to discuss briefly the width of the second phonon. In classical terms, the double excitation should have half the lifetime and therefore twice the width. This classical behavior can be derived from Fermi's Golden Rule under the assumption that the particles and holes of the two phonons do not interfere with each other in the matrix element mixing the 2p–2h double phonon with 3p–3h states. One may well ask, in the light of the coherence found for the decay of a single collective phonon, is the assumption justified? I will not go any further into this question, but just mention a recent calculation that finds some reduction in the width from twice the width of a single phonon [23].

7.2. *Hot fission*

With the ideas developed in the preceding lectures, we can take a look at fission of hot nuclei, the topic of Peter Paul's lectures. At very high energy, the nucleus will behave as a viscous liquid, and the rate at which it can change shape will depend on the coupling strengths between different degrees of freedom. This contrasts sharply with the behavior at low excitation. There the statistical theory

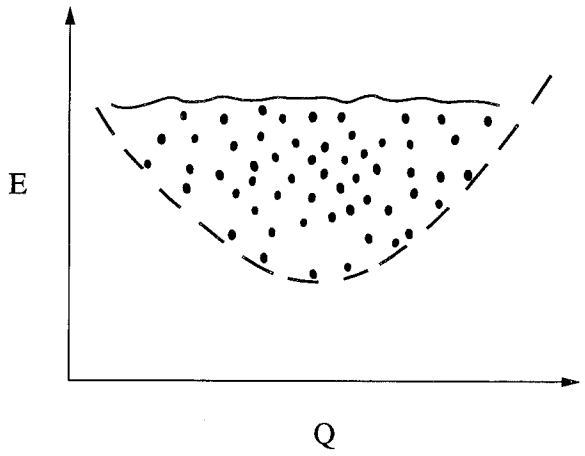

Fig. 12. Spectrum of self-consistent mean-field configurations.

of transition rates may be applied. The statistical decay rate depends only on the number of channels and the level densities; the dynamics becomes irrelevant.

To make a theory of the shape dynamics at high excitation energy we will go back to mean field theory, and assume that the mean field configurations are still a useful starting point for the further development. The distribution of mean field levels as a function of deformation is sketched in Fig. 12. Each mean field state is a self-consistent solution of the mean field equations, and may be characterized by its deformation and energy. These are the dots in the figure. At low excitation energy, the pairing mixes the mean-field configurations and this representation is less appropriate than the BCS description. The lower boundary of states in this plane describes the energy of a cold nucleus as a function of deformation. Let us consider the nucleus starting in some mean field state and ask how it evolves. The interactions mix nearby states, leading to a change in deformation. We can estimate the interaction rate using Fermi's golden rule,

$$\Gamma = 2\pi \langle i|v|f\rangle^2 \frac{dn}{d\epsilon}. \tag{7.5}$$

We will not try to evaluate eq. (7.5) from first principles, but just relate it to the empirical damping that we have already dealt with. A key part of this calculation will be to determine the density of states. We are dealing with a typical state at high excitation, so we will treat the single-particle occupation in an average way. The final state must have the same occupation factors as the initial state, except for the two particles that interact. These may jump from occupied orbitals to unoccupied orbitals. For a given orbital, the statistical factors that weight this are

the Fermi–Dirac factors f and $1-f$. We may then express the average density of final states as the integral

$$\frac{dn}{d\epsilon} = n_\epsilon^4 \int \Pi_i d\epsilon_i f_1 f_2 (1-f_3)(1-f_4)\delta(\epsilon_1+\epsilon_2-\epsilon_3-\epsilon_4).$$

This integral depends on temperature as T^3. To see this, change the energy variable to the dimensionless variable $x = \epsilon/T$ in the integral,

$$\frac{dn}{d\epsilon} = n_\epsilon^4 T^3 \int \Pi_i dx_i f_1 f_2 (1-f_3)(1-f_4)\delta(x_1+x_2-x_3-x_4).$$

Since the integrand depends only on the x the prefactor gives the entire T-dependence. The T^3 behavior can be understood qualitatively as follows. Each quasiparticle in the excited states has a width proportional to T^2, according to considerations we made earlier. The number of quasiparticles increases with temperature as T, and the total width increases as the number of quasiparticles times their width. At a temperature of 2.5 MeV, the single-particle width is of the order of 3 MeV, and the number of quasiparticles in a heavy nucleus is about 20. Thus the width of a single configuration at that temperature is about 60 MeV.

The width gives the rate at which the system moves from one configuration to another, but does not tell us directly how the deformation changes. However, it is possible to crudely estimate the number of configuration changes required to go from a spherical shape fission. The number of orbital changes required to go from a spherical mean-field state to a strongly deformed fission saddle configuration is of the order of the number of particles, A. I don't have time to derive this, but refer you to ref. [24]. Each two-particle interaction makes 4 orbital changes, so the number of interaction steps is better approximated by $A/4 \approx 50$. However, the motion of the nucleus from the spherical shape to the fission shape is a random walk over the energetically allowed configurations. Under these conditions the average distance the nucleus moves is the square of the number of steps times the step size. Combining this with the transition rate estimated in the previous paragraph, the time to go to fission comes out as

$$t = \frac{\hbar}{\Gamma}\left(\frac{A}{4}\right)^2 \approx 10^4 \text{ fm/c} = 3\times 10^{-20} \text{ s}$$

This is a very long time on the scale of neutron evaporation times, and is qualitatively in accord with the fission delay times found experimentally. However, this description gives too slow a rate at low temperature, because of the T^3 behavior of Γ. The treatment ignores pairing, which we saw gives collective motion at low frequency. It is an unsolved research problem to include pairing in the theory of fission at finite excitation energy.

Acknowledgment

This work was supported by the Department of Energy under Grant DE-FG06-90ER40561.

References

[1] J. Bacelar et al., Ed., *Proceedings of the Groningen Coherence on Giant Resonances*, Nucl. Phys. **A599** (1996).
[2] J. Speth and A. van der Woude, Rep. Prog. Phys. **44** (1981) 719.
[3] G.F. Bertsch and R.A. Broglia, *Oscillations in Finite Quantum Systems* (Cambridge Univ. Press, 1994).
[4] A. Bohr and B. Mottelson, *Nuclear Structure*, Vol. II (Benjamin, New York, 1975).
[5] P. Ring and P. Schuck, *The Nuclear Many-Body Problem* (Springer, Heidelberg, 1980).
[6] Y. Alhassid, M. Gai, and G.F. Bertsch, Phys. Rev. Lett. **49** (1982) 1282.
[7] O. Gunnarsson and B. Lundqvist, Phys. Rev. **B13** (1976) 4274.
[8] D. Vautherin and D. Brink, Phys. Rev. **C5** (1972) 626.
[9] P.H. Heenen, P. Bonche, and H. Flocard, Nucl. Phys. **A588** (1995) 490.
[10] J. Dobaczewski, W. Nazarewicz and T.R. Werner, Z. Phys. **A354** (1996) 27.
[11] J. Decharge and D. Gogny, Phys. Rev. **C21** (1980) 1568.
[12] M. Girod et al., Phys. Lett. **B325** (1994) 1.
[13] B. Serot and J. Walecka, Adv. Nucl. Phys. **16** (1986) 1.
[14] M.M. Sharma et al., Phys. Rev. Lett. **72** (1994) 1431.
[15] P. Dirac, Proc. Camb. Phil. Soc. **26** (1930) 376
[16] P. Bonche, S. Koonin and J. Negele, Phys. Rev. **C13** (1976) 1226.
[17] G.F. Bertsch and H. Feldmeier, Phys. Rev. **C56** (1997) 839.
[18] O. Bohigas, A. Lane and J. Martorell, Phys. Rep. **51C** (1979) 267.
[19] H. Steinwedel and J. Jensen, Z. Naturforschung **8** (1950) 413.
[20] D. Bohm and D. Pines, Phys. Rev. **92** (1953) 609.
[21] M. Rein et al., Phys. Rev. **C49** (1994) 250.
[22] H. Esbensen and G.F. Bertsch, Ann. Phys. **157** (1984) 255.
[23] V. Ponomarev et al., Z. Phys. **A356** (1996) 251.
[24] G.F. Bertsch, Phys. Lett. **95B** (1980) 157.
[25] G. Bertsch and H. Flocard, Phys. Rev. **C43** (1991) 2200.
[26] P. Bonche et al., Nucl. Phys. **A510** (1990) 466.
[27] M. Brack et al., Rev. Mod. Phys. **44** (1972) 320.
[28] A. Fetter and J. Walecka, *Quantum Theory of Many-Particle Systems* (McGraw Hill, New York, 1971).
[29] J.P. Blaizot, Phys. Rep. **64** (1980) 171.
[30] J.P. Blaizot et al., Nucl. Phys. **A591** (1995) 435.
[31] M. Deleze et al., Nucl. Phys. **A554** (1993) 1.
[32] M. Yeh et al., Phys. Rev. Lett. **76** (1996) 1208.
[33] R. Schmidt et al., Phys. Rev. Lett. **70** (1993) 1767.
[34] J. Ritman et al., Phys. Rev. Lett. **70** (1993) 533.
[35] J. Stroth et al., Nucl. Phys. **A599** (1996) 307c.
[36] G. Lalazissis, private communication.
[37] G. Bertsch, P. Bortignon, and R. Broglia, Rev. Mod. Phys. **55** (1983) 287.